BNL-47242
Informal Report

DEMONSTRATION OF RAPID AND SENSITIVE MODULE LEAK CERTIFICATION FOR SPACE STATION FREEDOM

FINAL REPORT

R. N. DIETZ AND R. W. GOODRICH

MARCH 1991

DEPARTMENT OF APPLIED SCIENCE

BROOKHAVEN NATIONAL LABORATORY
UPTON, LONG ISLAND, NEW YORK 11973

DISCLAIMER

BNL--47242

DE92 014168

DEMONSTRATION OF RAPID AND SENSITIVE MODULE LEAK CERTIFICATION FOR SPACE STATION FREEDOM

FINAL REPORT

Russell N. Dietz and Robert W. Goodrich
Tracer Technology Center
Brookhaven National Laboratory
Upton, NY 11973

March 1991

Prepared for the
Marshall Space Flight Center
Huntsville, AL 35812

UNDER CONTRACT NO. DE-AC02-76CH00016 WITH THE
UNITED STATES DEPARTMENT OF ENERGY

CONTENTS

CONTENTS (Continued)

ABSTRACT

A leak detection and quantification demonstration using perfluorocarbon tracer (PFT) technology was successfully performed at the NASA Marshall Space Flight Center on January 25, 1991. The real-time Dual Trap Analyzer (DTA) at one-half hour after the start of the first run gave an estimated leak rate of 0.7 mL/min. This has since been refined to be 1.15 ± 0.09 mL/min. The leak rates in the next three runs were determined to be 9.8 ± 0.7, -0.4 ± 0.3, and 76 ± 6 mL/min, respectively.

The theory on leak quantification in the steady-state and time-dependent modes for a single zone test facility was developed and applied to the above determinations.

The laboratory PFT analysis system gave a limit-of-detection (LOD) of 0.05 fL for ocPDCH,. This is the tracer of choice (Appendix A), and is about 100-fold better than that for the DTA. Applied to leak certification, the LOD is about 0.00002 mL/s (0.000075 L/h), a 5 order-of-magnitude improvement over the original leak certification specification (Appendix B). Furthermore, this limit can be attained in a measurement period of 3 to 4 hours instead of days, weeks, or months. A new Leak Certification Facility is also proposed to provide for zonal (three zones) determination of leak rates. The appropriate multizone equations, their solutions, and error analysis have already been derived.

Permeation of tracer through elastomeric seals on the module is not of concern (Appendix C).

A new concept of seal-integrity certification has been demonstrated for a variety of controlled leaks (Appendix D) in the range of module leak testing. High structural integrity leaks were shown to have a linear dependence of flow on Δp (a power dependency of 1.0); poor integrity leaks exhibited a power dependency of 1.5 to 2.5. The rapid determination of leak rates at different pressures is proposed and is to be determined while subjecting the module to other external force-generating parameters such as vibration, torque, solar intensity, etc.

INTRODUCTION

The previous leak detection specification of 2 mL/second (120 mL/min, 7.2 L/h, or 0.47 lbs/day) at a Δp of 1 atm (14.7 psig or 760 torr gage) for the Space Station Freedom (SSF) module leak certification testing, which was to have been performed by pressure decay, would, on average, have required about 10 to 30 days per module using the planned Boeing system[1] or 2.5 to 8 days per module under their improved plan to achieve the desired accuracy of about ±1%.

Brookhaven corroborated the pressure decay calculations, estimating that precision would be about ±5% under the proposed test conditions[2], but then calculated that, by using perfluorocarbon tracer (PFT) technology[3], the testing duration required for a precise (to about ±10%) leak rate determination could be substantially shortened while simultaneously detecting orders-of-magnitude smaller leaks.[2] Estimates of testing times were:

	Required Testing Duration		
Leak rate spec., mL/s:	2	0.002	0.0002
Pressure decay:	2-30 days	decades	centuries
PFT @ 0.1 ppm:	4 seconds	1 h	8 h
PFT @ 10 ppm:	40 ms	0.5 min	5 min

The times indicated were the anticipated tracer sampling duration after the module leak testing room had come to steady state, which is itself a process that takes an hour or more depending on air flow rate. For real-time sampling and analysis, the dual-trap analyzer[4] with its present cycle time of 6 min (0.1 h) would require 30 min of operation in a single zone to have sufficient data (5 points) to calculate the leak rate from the tracer model, even if the testing facility had not yet reached steady state.

These calculations implied that SSF module leak certification would be markedly enhanced by the PFT approach. To confirm the Brookhaven-proposed method, a test was conducted on January 25, 1991, at the Building 4572 test facility of the Marshall Space Flight Center (MSFC). The results from this testing are presented here, confirming that the potential for module leak certification is even an order-of-magnitude better than anticipated. Further, a new proposed concept of seal-integrity certification determined by the leak rate's dependence on module pressure differential, a unique feature of the PFT approach, should significantly enhance safety and reliability.

EXPERIMENTAL

SURROGATE MODULE TEST DEVICE

Engineers from the Structures/Mechanisms test group of the Boeing Defence and Space Group prepared a small test cell (about 10 L) equipped with one of two mass-flow controllers which could be operated from 0 to 10 and 0 to 100 mL/min, respectively. Once pressurized with N_2 containing about 4 ppm (μL/L) of ocPDCH (ortho-cis-perfluorodimethylcyclohexane), which filling was performed just outside the building, the surrogate module test device was then set in about the middle of the long wall of the ~4000-m^3 volume building and about one-third the way from the wall. A floor fan was placed about two-thirds the way across the room (about 15-feet from the test device), blowing away from the device to facilitate PFT mixing into the air in the room.

PFT EQUIPMENT

On a table just upwind from the "leaking" surrogate module, Brookhaven placed the real-time Dual Trap Analyzer (DTA) and one programmable sampler (Brookhaven Atmospheric Tracer Sampler - BATS); another BATS was placed across the room, downwind of the fan, to serve both as a back-up to the first as well as to check on the uniformity of tracer concentrations. In addition, passive samplers were placed at several locations around the room, in part to further corroborate tracer concentrations and also to see if proximity to the leak could be detected. Since, as will be explained later, the room was accidently overdosed with tracer at one point, no useful results could be obtained from the passive samplers.

Dual Trap Analyzer (DTA)

The DTA was set to a cycle time of 6 minutes. While one of the two adsorbent traps was being thermally desorbed and analyzed on the in situ gas chromatograph system, the other was sampling air at a rate of 0.207 L/min (a high flow rate of 2.135 L/min was also available but the traps are not 100% efficient at that rate); the high flow rate was used for only a few analyses. At the end of the 6-min cycle, the traps switched and the process was repeated. For this test, the output information was displayed only on a strip chart recorder. Measurement of tracer quantity was obtained from hand measurements of peak heights (voltage) which was subsequently calibrated versus quantity of tracer back in the laboratory.

Programmable Samplers

The programmable samplers (BATS) contains 23 sampling tubes in its lid assembly and a pump, internal clock, etc.,.in its base assembly.[3] During operation, air was pulled at a known rate (in this case nominally 50 mL/min) through the adsorbent in the sampling tube, retaining essentially all of the PFTs for subsequent thermal desorption and analysis in the laboratory.

The unit next to the DTA (analysis file 7337B) collected 15-min samples starting at 0900 and the unit across the room (analysis file 7338B) started at 0915. At 1100, the start of the first intentional leak from the surrogate module, the sampling duration was changed to 10-min intervals. Thus, the BATS units finished collecting samples at 1330 and 1340, respectively, before the start of the fourth run; run no. 4 was only analyzed by the DTA. The BATS were returned to Brookhaven for analysis on the laboratory gas chromatograph (GC) system. Details on the calibration and operation of the GC are provided elsewhere.[3]

Tracer Sources

As indicated earlier, the surrogate module device was filled with N_2 containing about 4 ppm of ocPDCH, the "leaking" tracer. The small cylinder brought to the test site was prepared by dilution from a 10-fold higher concentration standard and subsequently corroborated at BNL.

The "reference" tracer sources, small permeation capsules of known source rate[5], were deployed adjacent to the point of emanation of the leaking tracer. Basically, by measuring the ratio of the leaking tracer concentration to reference tracer concentration in the air at steady state and knowing the reference tracer rate, the leak rate can be directly calculated. Two reference tracers were used, PMCP (perfluoromethylcyclopentane) and ptPDCH (para-trans-perfluorodimethylcyclohexane), one as a back-up in case of analytical problems.

TEST PROCEDURES AND CONDITIONS

The BNL equipment was brought to Building 4572 at about 0730 and the DTA started operation around 0800 while other equipment was being readied. The BATS near the DTA was started at 0900 and the one across the room (opposite the DTA), at 0915, collecting 15-min samples which, initially, should have been ambient background levels.

At exactly 0930, the reference PFT tracers were deployed in the building at the surrogate-module leak site; this provided time for the reference tracer concentration to reach steady state before the first leak run began. During this period, outside the building, about 20 feet away from a door, on its upwind side, the surrogate module was being filled with the "leaking" tracer source gas; this should have been done downwind of the building and at least 50 feet away as will be shown later. At 1030, the surrogate module was brought into the building and set up at the leak site.

A summary of test conditions is as follows:

Time	Event
0800	DTA operating and BATS deployed
0900	BATS near DTA started (15-min samples)
0915	BATS across room (opposite DTA) started (15-min samples)
0915 to 0945	Surrogate module filled with "leaking" tracer-tagged N_2
0930	PFT reference sources deployed at leak site
1030	Surrogate module deployed at leak site
1100	BATS units both switched to collecting 10-min samples
1100 to 1130	Run no. 1 leak rate set with 0-10 mL/min transducer
1130 to 1200	Run no. 2 leak rate set with 0-10 mL/min transducer
1200 to 1230	Run no. 3 leak rate set with 0-10 mL/min transducer
1233 to 1236	Surrogate module brought outside and vented
1240 to 1300	0-100 mL/min transducer installed on surrogate module
1326 to 1330	Building ventilated with wall fans
1340 to 1350	Surrogate module refilled with "leaking" tracer-tagged N_2
1355	Surrogate module deployed at leak site
1404 ~ 1443	Run no. 4 leak rate set with 0-100 mL/min transducer

Right after the first run started at 1100, the BATS units were switched to collect 10-min samples, which allowed 3 samples to be collected during each of the one-half hour runs. The flow rate for run no. 1 was obviously set to a value between 0 and 10 mL/min (the range covered by the transducer), but the

Brookhaven personnel did not know the setting. The other two runs commenced exactly at the times indicated. Once adjusted, the "leak rate" was left constant for the duration of the run.

The Brookhaven personnel were not present when the surrogate module was vented just outside the building shortly after 1230 in order to switch to the 0-100 mL/min flow transducer. The DTA and BATS units' analysis data clearly showed that the dumping occurred sometime between 1233 to 1236; both the DTA sample collected from 1231 to 1237 and the BATS data from 1230 to 1240 showed a positive deviation from the trend of decreasing concentration of leaking tracer with time which occurred during run no. 3.

On return and assessing the impact as revealed by the DTA, the building was ventilated for about one-half hour using its own large near-roof wall fans. During this period, the surrogate module was recharged with the leaking tracer, the device was set up at the leak site, the fans were turned off, and run no. 4 commenced at about 1404 until about 1443; the exact time that the leak was shut down was not known by Brookhaven.

UNITS USED TO EXPRESS TRACER CONCENTRATIONS

The levels at which PFT concentrations are routinely measured at Brookhaven are quite low and the units used to express those values may be unfamiliar to some readers. The table below expresses this nomenclature:

Tracer Concentration Nomenclature

Tri-decade Level	Parts per	Other Units		
10^{-3} to 10^{-6}	million - ppm	nL/mL	µL/L	mL/m^3
10^{-6} to 10^{-9}	billion - ppb	pL/mL	nL/L	$\mu L/m^3$
10^{-9} to 10^{-12}	trillion - ppt	fL/mL	pL/L	nL/m^3
10^{-12} to 10^{-15}	quadrillion -ppq		fL/L	pL/m^3

where

L = liters (1000 L = 1 m^3)

mL = milliliter (10^{-3} liter)

μL = microliter (10^{-6} liter)

nL = nanoliter (10^{-9} liter)

pL = picoliter (10^{-12} liter)

fL = femtoliter (10^{-15} liter)

Thus, for example, the PFT emission rate from the surrogate module can be calculated from its known concentration (about 4 ppm) and its known flow rate (say 10 mL/min) by choosing the proper units:

$$C = 4 \text{ ppm} = 4 \text{ nL / mL}$$
$$R = 10 \text{ mL / min} = 600 \text{ mL / h}$$
$$S = CR = 4 \frac{\text{nL}}{\text{mL}} \times 600 \frac{\text{mL}}{\text{h}} = 2400 \text{ nL / h}$$

The present background ambient air levels of the 4 PFTs used in this study are:

PFT	Background Conc., fL/L	Use
PMCP	3.3 ± 0.1	Reference tracer
PMCH	3.5 ± 0.2	Present in leaking tracer
ocPDCH	0.25 ± 0.02	Leaking tracer
ptPDCH	4.6 ± 0.2	Reference tracer

THEORY ON LEAK QUANTIFICATION WITH TRACERS

As indicated earlier, the quantification of an unknown leak rate source can be obtained very simply from the product of the known reference tracer source rate and the ratio of the leaking tracer to reference tracer -- **when the test scenario is at steady state.**

Figures 1 to 4 show the ratio of the concentrations of the leaking tracer, ocPDCH, to the reference tracer, ptPDCH, versus the time of the day from the analysis results of the two programmable samplers (BATS) and the real-time DTA, both the morning and the afternoon runs. Clearly, since the reference tracer concentration had been at steady state prior to starting the runs, the leaking tracer concentration had not achieved steady-state levels in any of the runs, that is, rise to a level and then remain at the constant level for some time (steady state) before the next change was made. This has required a more complicated solution to the differential equation defining the test.

A simple material balance around Building 4572, assuming a constantly emitting "reference" (r) tracer source is located within, yields

$$\frac{dv_r(t)}{dt} = S_r - R_E(t)\frac{v_r(t)}{V_B} \tag{1}$$

where $v_r(t)$ is the volume (nL, nanoliters or 10^{-9} liters) of reference tracer gas present in the building at any time t(h), S_r is the reference tracer source rate (nL/h), $R_E(t)$ is the building air exfiltration rate which may vary with time (m^3/h), and V_B is the volume of the building (m^3). Rearranging gives

$$R_E(t) = \frac{V}{v_r(t)}\left(S_r - dv_r(t)/dt\right)$$

$$= S_r \frac{V_B}{v_r(t)}\left(1 - \frac{dv_r(t)/dt}{S_r}\right)$$

$$= \frac{S_r}{C_r(t)}\left(1 - \frac{dC_r(t)/dt}{S_r/V_B}\right) \tag{2}$$

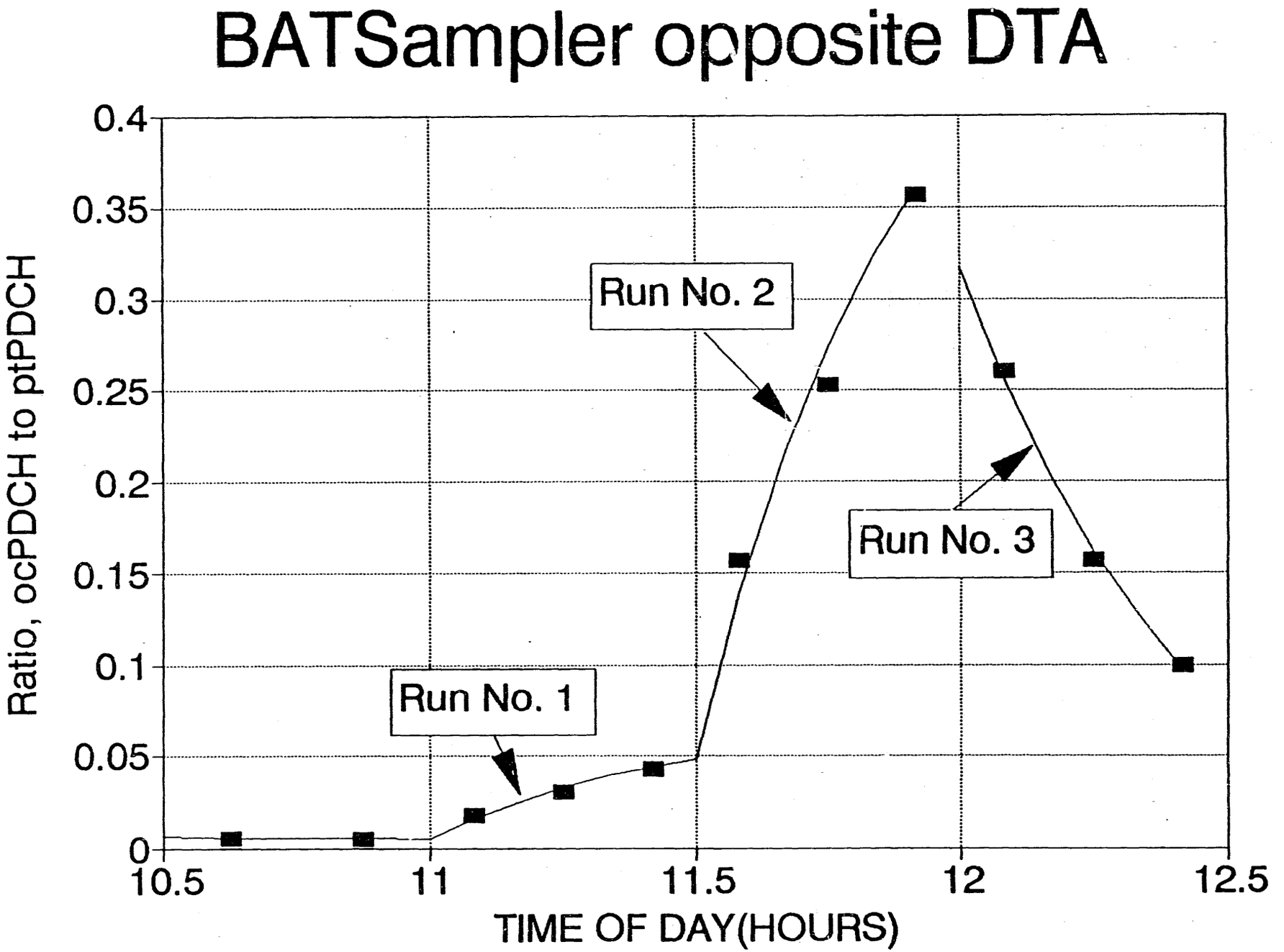
BATSampler opposite DTA
Ratio, ocPDCH to ptPDCH
0.4
0.35
0.3
0.25
0.2
0.15
0.1
0.05
0
10.5
11
11.5
12
12.5
TIME OF DAY(HOURS)
Run No. 1
Run No. 2
Run No. 3

Figure 1

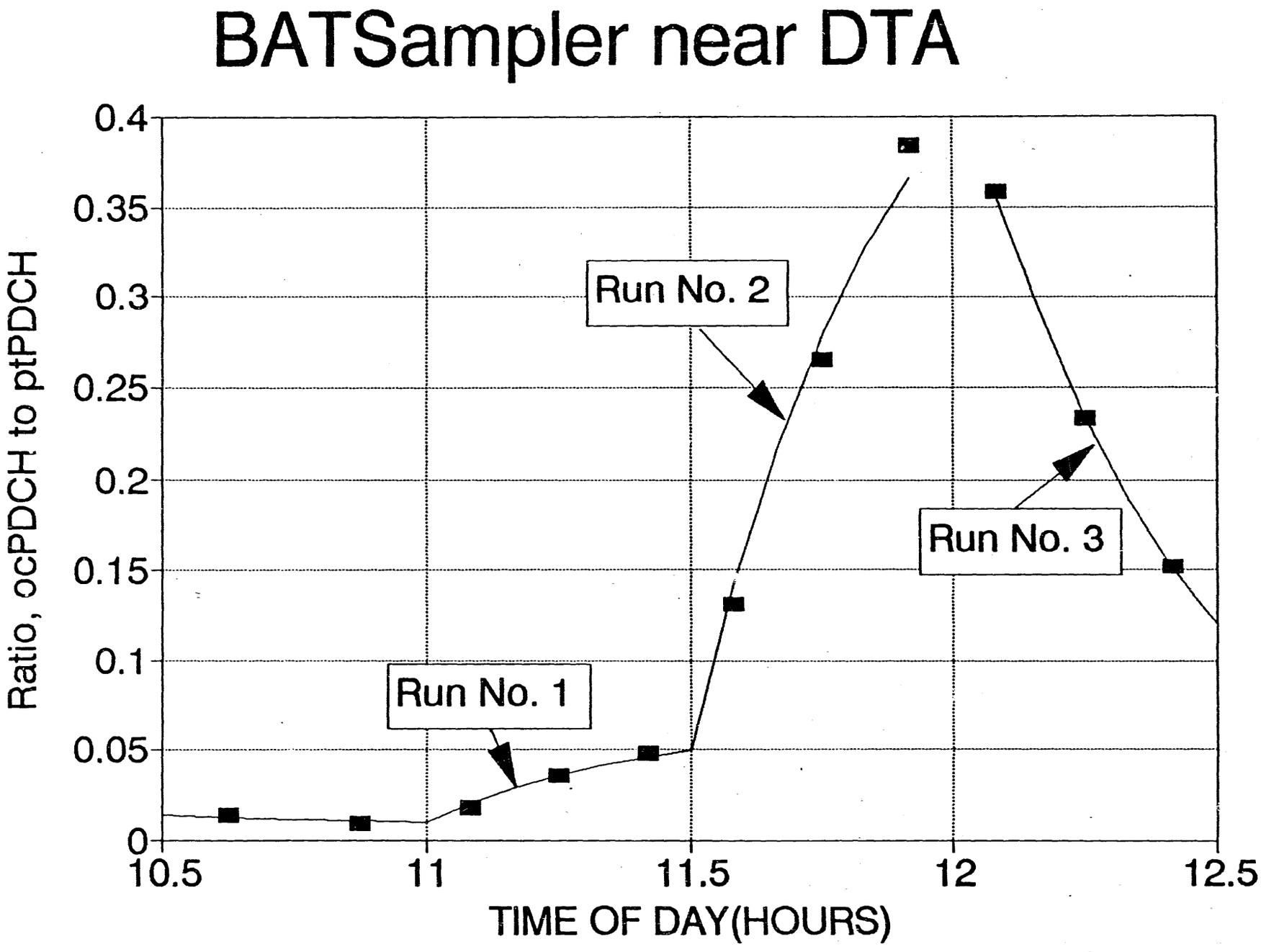
BATSampler near DTA
Ratio, ocPDCH to ptPDCH
0.4
0.35
0.3
0.25
0.2
0.15
0.1
0.05
0
10.5
11
11.5
12
12.5
TIME OF DAY(HOURS)
Run No. 1
Run No. 2
Run No. 3

Figure 2

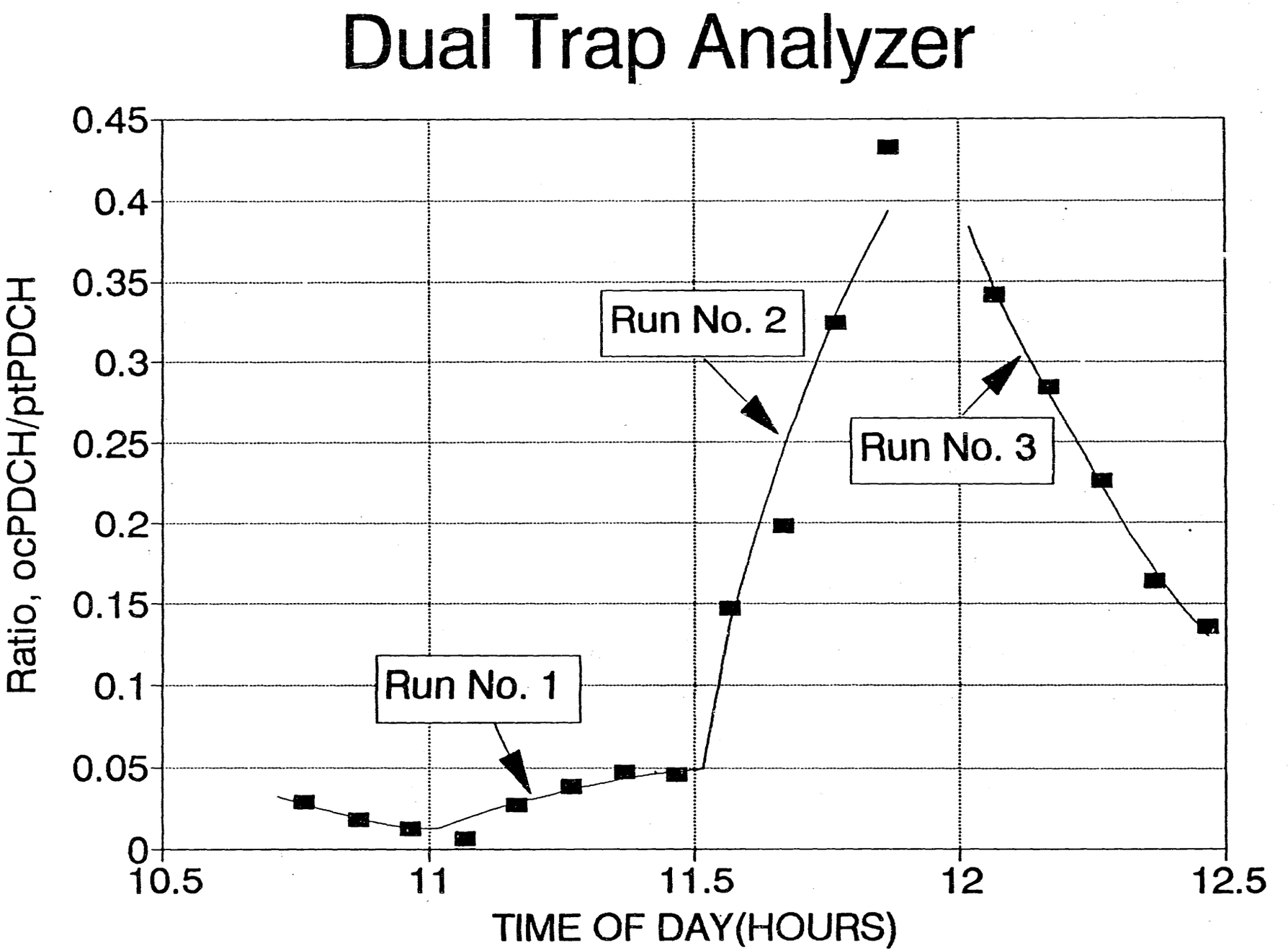
Dual Trap Analyzer
Ratio, ocPDCH/ptPDCH
0.45
0.4
0.35
0.3
0.25
0.2
0.15
0.1
0.05
0
10.5
11
11.5
12
12.5
TIME OF DAY(HOURS)
Run No. 1
Run No. 2
Run No. 3

Figure 3

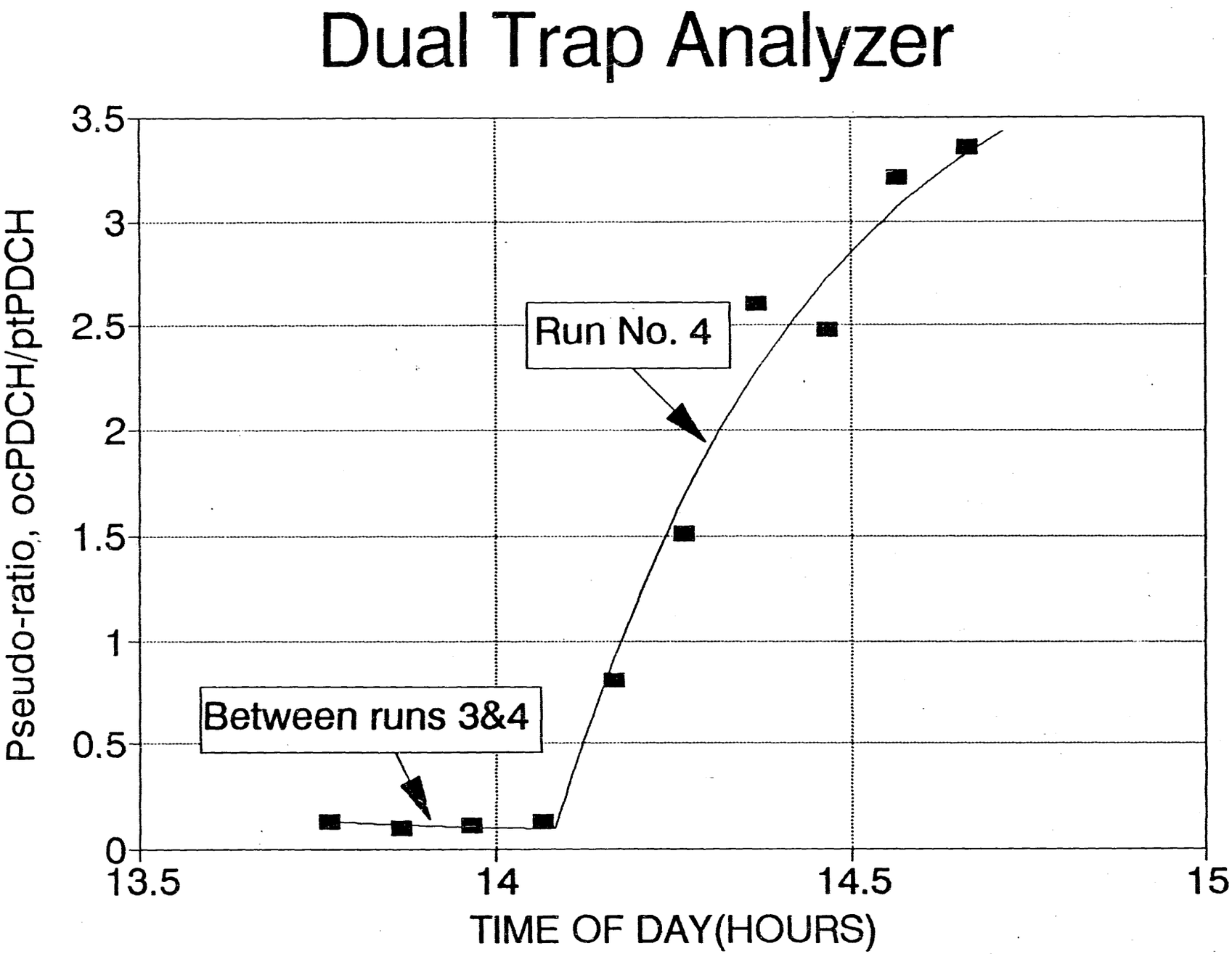
Dual Trap Analyzer
Pseudo-ratio, ocPDCH/ptPDCH
3.5
3
2.5
2
1.5
1
0.5
0
13.5
14
14.5
15
TIME OF DAY(HOURS)
Run No. 4
Between runs 3&4

Figure 4

where $C_r(t)$ is the time-dependent reference tracer concentration, equivalent to $v_r(t)/V_B$.

If, within the building, a module is leaking air containing a different type "leaking" tracer (ℓ) a similar equation can be written

$$R_E(t) = \frac{S_\ell}{C_\ell(t)}\left(1 - \frac{dC_\ell(t)/dt}{S_\ell / V_B}\right) \tag{3}$$

It can be shown that, since the same exfiltration rate is governing the time-dependent performance of both tracers, Eqs. (2) and (3) can be set equal to each other and solved for the source rate of the leaking tracer giving

$$S_\ell = S_r \frac{C_\ell(t)}{C_r(t)} - V_B \frac{C_\ell(t)}{C_r(t)} dC_r(t)/dt + V_B\, dC_\ell(t)/dt \tag{4}$$

Finally, the air leakage rate of the module, R_ℓ (mL/h), is the calculated module tracer source rate, S_ℓ (nL/h), divided by the known tracer concentration, C_{mi} (nL/mL), within the module, that is

$$R_\ell = \frac{S_\ell}{C_{mi}} \tag{5}$$

where C_{mi} is the concentration (nL/mL is equivalent to mL/L or parts per million) inside the module, a known value.

STEADY-STATE SOLUTION

As shown in Figures 1 to 4, within one-half hour after a change in the rate of the surrogate-module leak, the tracer concentration had not equilibrated when the next change occurred. It can be shown that the time required to reach 95 to 98% of the steady-state concentration is 3 to 4 times the time, τ(h), for one complete change of air in the building. From the reference tracer data, τ was found to be 0.40 ± 0.03 h; thus, steady state would not be achieved until 1.2 to 1.6 h after a change, and certainly not in the 30 min of each of the four (4) runs conducted in January.

If steady state had been attained for the leaking tracer, then $dC_\ell(t)/dt$ would have been zero and, since the reference tracer was at steady state (the reference tracer was brought into the building at 0930 and the first run began at 1100), $dC_r(t)/dt$ was zero, then Eq. (4) simplifies to

$$S_\ell = S_r \frac{C_\ell}{C_r} \tag{6}$$

where C_ℓ and C_r are the leaking and reference tracer concentrations (nL/m^3) at steady state, respectively. Substituting into Eq. (5) gives

$$R_\ell = \frac{C_\ell S_r}{C_r C_{mi}} \tag{7}$$

Equation (7) can be used to calculate estimated leak rates (even though not at steady state) for comparison to the more precisely determined values. An example is the calculation made for the estimated leak rate for Run No. 1 on the day of the test from the real-time DTA data. C_ℓ from the last analysis of that period (mid-time was 11:28) was 0.0101 nL/m^3 and the steady-state reference tracer concentration, C_r, was 0.208 nL/m^3. Since the reference source rate, S_r, was 82.5 nL/min and the concentration, C_{mi}, of the ocPDCH inside the surrogate module was 4.27 nL/mL (ppm), Eq. (7) gives

$$R_\ell = \frac{(0.0101)(82.5)}{(0.208)(4.27)} = 0.94 \text{ mL/min}$$

which is close to the best determination of the true value.

TIME-DEPENDENT SOLUTIONS

Since the data clearly showed that the concentration of the leaking tracer was varying throughout each of the four runs, the source rate of the leaking tracer, S_ℓ, should be determined from the best fit to all the data available in a given period. This can be accomplished in two ways -- a derivative fit and an integral fit. In addition, the building volume, V_B, and the air turnover time, τ, can be determined from the initial reference tracer data.

Derivative Fit

The derivatives for the reference and leaking tracers in Eq. (4) can be estimated for each point by calculating the slope at each point from the actual ocPDCH concentration versus time data (similar to the data of Figs. 1 to 4). Using the differential of Stirling's formula for a smoothly changing function expressed in terms of differences which are in the same horizontal line[6] and assuming that higher order terms are not significant, it can be shown[7] that

$$\frac{dC(t_2)}{dt} = \frac{C(t_3) - C(t_1)}{t_3 - t_1} \tag{8}$$

for the case when the sampling time intervals are equal.

However, at the beginning and the end of each run, there is an abrupt change in the function because the leak rate was changed. Thus, for the first point on the new function, the slope must be estimated from the first two points and, for the last point, from the last two points. It can be shown that

$$\frac{dC(t_1)}{dt} = \frac{C(t_2) - C(t_1)}{(t_2 - t_1)\ 0.75} \tag{9}$$

and

$$\frac{dC(t_n)}{dt} = \frac{C(t_n) - C(t_{n-1})}{(t_n - t_{n-1})\ 1.23} \tag{10}$$

where n is the last point in the current region. The estimates of the constants in Eqs. (9) and (10) were obtained by estimating slopes from the curves for some of the data. The same procedure applied to non-end points showed that Eq. (8) estimated the true slope, on average, to within better than ±1%.

For all the data collected by either the DTA or the BATS units, the derivative of the reference tracer was calculated by Eq. (8) and that for the leaking tracer, either by Eqs. (8), (9), or (10) depending on location. Eq. (4) can then be solved for S_ℓ by substituting the appropriate derivative values along with S_r, the known reference tracer rate, $C_\ell(t)/C_r(t)$, the known ratio of the concentrations of ocPDCH

to ptPDCH, and the volume of the building, V_B. This volume can be estimated from the physical volume or derived from the tracer data as shown in the later section so named.

Integral Fit

Another solution to Eq. (4) can be obtained by assuming that the change in the reference tracer concentration with time is small and can be neglected. Thus, Eq. (4) becomes

$$S_\ell = S_r \frac{C_\ell(t)}{C_r(t)} - V_B \, dC_\ell(t)/dt$$

which, on rearranging, gives

$$\frac{dC_\ell(t)}{\frac{S_\ell}{S_r}C_r(t) - C_\ell(t)} = \frac{S_r}{V_B}\frac{dt}{C_r(t)} \qquad (11)$$

Because the reference tracer concentration is at steady state, $C_r(t)$ is essentially constant, i.e., $C_r(t) = C_r$. Then, integrating Eq. (11) from an initial time, t_o, at which $C_\ell(t)/C_\ell(t_o)$, to a later time, t_a, at which, $C_\ell(t)/C_\ell(t_a)$ gives

$$\ln \frac{\frac{S_\ell}{S_r}C_r - C_\ell(t_o)}{\frac{S_\ell}{S_r}C_r - C_\ell(t_a)} = \frac{S_r}{V_B C_r}(t_a - t_o)$$

Taking the exponential of both sides, rearranging, and solving for the concentration of the leaking tracer at any time, t_a, gives

$$C_\ell(t_a) = \frac{S_\ell}{S_r}C_r - \left[\frac{S_\ell}{S_r}C_r - C_\ell(t_o)\right] e^{-\frac{S_r}{V_B C_r}(t_a - t_o)} \qquad (12)$$

The quotient in the exponential can be simplified by

$$V_B = R_E \, \tau$$

which, by definition, says that the volume (m^3) of the building divided by the rate (m^3/h) of air exfiltration is the air turnover time, τ(h), and

$$R_E = S_r/C_r$$

which is obtained from Eq. (2) for the reference tracer at steady state. Thus, the quotient becomes

$$\frac{S_r / C_r}{V_B} = \frac{S_r / C_r}{R_E \tau} = \frac{S_r / C_r}{\tau S_r / C_r} = \frac{1}{\tau}$$

Substituting into Eq. (12), dividing both sides by C_r, and letting the concentration ratio of leaking to reference tracer be

$$C'_\ell(t_a) = C_\ell(t_a) / C_r$$

gives

$$C'_\ell(t_a) = \frac{S_\ell}{S_r} - \left[\frac{S_\ell}{S_r} - C'_\ell(t_o)\right] e^{-(t_a - t_o)/\tau} \tag{13}$$

where τ is the average turnover time for each run period; the determination of τ is described in the next section.

Eq. (13) is the function representing the smooth curve drawn on Figs. 1 to 4 for each of the distinctly different periods of different surrogate-module tracer leak rate, S_ℓ, and the integral of the function from one time (t_{a1}) to another (t_{a2})

$$\text{Area} = \int_{t_{a1}}^{t_{a2}} C'_\ell(t_a) dt_a = \frac{S_\ell}{S_r}(t_{a2} - t_{a1}) + \tau\left[\frac{S_\ell}{S_r} - C'_\ell(t_o)\right]\left[e^{-(t_{a2} - t_o)/\tau - (t_{a1} - t_o)/\tau}\right]$$

represents the area under the curve between the two times. But this area is also precisely the average tracer concentration ratio measured by the samplers times the time interval, i.e.,

$$\text{Area} = \overline{C}'_\ell(t_{a2} - t_{a1})$$

Equating the two, dividing by (t_{a2}-t_{a1}), and solving for S_ℓ/S_r gives

$$S_\ell/S_r = \overline{C}'_\ell \Big|_{t_{a1}}^{t_{a2}} - \frac{\tau\left[(S_\ell/S_r) - C'_\ell(t_0)\right]}{t_{a2} - t_{a1}}\left[e^{-(t_{a2} - t_0)/\tau} - e^{-(t_{a1} - t_0/\tau)}\right] \tag{14}$$

where $\overline{C}'_\ell \Big|_{t_{a1}}^{t_{a2}}$ is the ocPDCH ratio from the analysis of a single sample collected from t_{a1} to t_{a2} or the average of several consecutive samples over the time period of the consecutive samples.

The solution of Eq. (14) for a particular run is effectively the best fit of the data for the assumed τ, starting with a best estimate of $C'_\ell(t_o)$ obtained from the data prior to the first run. Equation (14) is solved by an iterative calculation, assuming a value for S_ℓ/S_r and then calculating a value until the result converges. By solving Eq. (14) over the entire 30-min period of a run, the best value of S_ℓ/S_r is obtained which, multiplying by the known S_r value and substituting into Eq. (5) gives the surrogate-module leak rate. Similarly, solving Eq. (14) over each of the individual sample periods provides an estimate of the uncertainty on the overall fit.

Building Volume and Turnover Time

The data from the initial buildup of the reference tracer concentration which started at 0930 can be used to calculate the volume of the building, V_B, and the air turnover time, τ. Since, for short periods (1 to 2 h), the exfiltration rate can be considered constant, i.e., $R_E(t) = R_E$, Eq. (1) can be integrated, yielding, for an initial reference tracer concentration of zero,

$$C_r(t) = \frac{S_r}{R_E}\left(1 - e^{-t/\tau}\right) \tag{15}$$

where, as before, τ is V_B/R_E. The exponential expansion of Eq. (15) is

$$C_r(t) = \frac{S_r}{R_E}\left(\frac{t}{\tau} - \frac{1}{2}\frac{t^2}{\tau^2} + \frac{1}{6}\frac{t^3}{\tau^3} - \ldots\right)$$

which, for short times ($t/\tau < 0.5$), can be approximated by just the first two terms of the expansion. Dividing by τ and factoring gives

$$\frac{C_r(t)}{t} = \frac{S_r}{R_E\tau}\left(1 - \frac{t}{2\tau}\right) = a - bt \tag{16}$$

which is the equation for a straight line. Since

$$a = \frac{S_r}{R_E \tau} = \frac{S_r}{V_B} \tag{17}$$

Eq. (17) can be used to calculate the volume of the building from the intercept since S_r is known. Also, from Eq. (16),

$$\frac{a}{b} = 2\tau \tag{18}$$

Thus, Eq. (18) can be used to calculate τ from the slope and the intercept.

To use the data collected for time greater than t/τ of 0.5 (which, in this study, since τ was about 0.4 h, meant the maximum t would be 0.2 h or 12 min, i.e., only one 10-min BATS sample or two 6-min DTA samples), it was shown[7] that an adjusted $C_r(t)/t$ value can be used to give

$$\text{Adjusted } \frac{C_r(t)}{t} = \frac{C(t)}{t} - a\left[\left(1 - e^{-t/\tau}\right)\frac{\tau}{t} + \frac{1}{2}\frac{t}{\tau} - 1\right]$$

$$= a - bt \tag{19}$$

The first two or three data points are used in Eq. (16) to obtain estimates of a and τ, which are then substituted into Eq. (19) to calculate an adjusted $C_r(t)/t$, which is then plotted versus time to obtain better estimates of a and τ. Repeated calculations result in a unique solution for τ, from Eq. (18), and V_B, from Eq. (17), and their uncertainties. The values of τ and V_B can then be used in the integral and derivative solutions, respectively, for the surrogate-module leak rate determinations.

RESULTS AND DISCUSSION

This section presents the results of the calibration of the DTA, the analytical corroboration of the leaking tracer concentration and the composition of the reference tracer, the DTA and BATS analyses from the January 25, 1991, test, and the computation of the building volume and the surrogate-module leak rates for the four test runs.

DTA CALIBRATION

A gas standard was prepared by placing gravimetrically calibrated permeation-type PFT sources into a 2.70-L plastic container for a known period of time at a known temperature to produce a known concentration mixture of the following tracers:

PFT Type	PMCP	PMCH	ocPDCH	ptPDCH
Rate for 1 @ 22°C, nL/min	32.8	17.2	5.52	8.25
No. of sources	1	2	4	6
Time in container, min	25 sec	1	1	1
Concentration, pL/mL	5.06	12.73	8.18	18.33
Elution time, min	1.55	2.35	3.8	5.4

Using syringes, aliquots of the above mixture from 0.01 to 10 mL were injected into the DTA; at least two samples of the same size were analyzed consecutively so that both traps A and B would be calibrated (the response of each is slightly different). A typical chromatographic response is shown in Figure 5 for a 0.1 mL sample of a similar, but slightly different mixture. The four PFT peaks are clearly shown; that labeled PMES is actually a combination of otPDCH and pcPDCH, the other isomer "halves" of the ortho- and para-PDCH tracers which are not quantified because they are not separately resolved.

The complete results of the calibration performed on February 12, 1991, are shown in Table 1. For each PFT, its quantity, v(pL), response height, H (volts), and height-to-quantity ratio, H/v (V/pL), are tabulated for each sample analyzed. The calibration curve is linear up to slightly over 2 volts (i.e., about 20 pL) when H/v is plotted versus H as shown by an example for ocPDCH on trap B (cf. Figure 6).

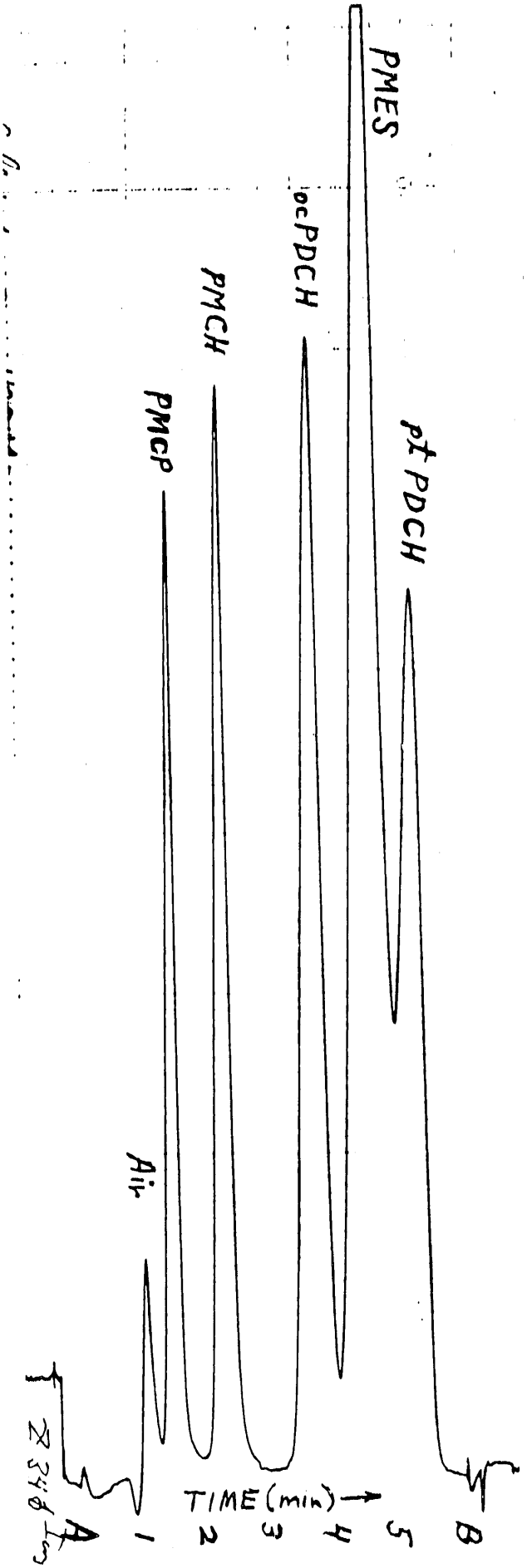

Figure 5. DTA response to 0.1 mL sample of a PFT standard.

Table 1.

DTA Calibration of 2/12/91

TRAP	TIME Inj.	ANAL.	SAMPLE VOL.,ml	PMCP QTY,pL	PMCP Ht,volts	PMCP H/v,V/pL	PMCH QTY,pL	PMCH Ht,volts	PMCH H/v,V/pL	ocPDCH QTY,pL	ocPDCH Ht,volts	ocPDCH H/v,V/pL	ptPDCH QTY,pL	ptPDCH Ht,volts	ptPDCH H/v,V/p
	14:15														
A	15:37	15:42	0.01	0.0466164	0.0228	0.489099	0.117278	0.0208	0.177356	0.07536	0.024	0.318471	0.168869	0.0186	0.11014
A	15:25	15:30	0.03	0.1415374	0.0659	0.465601	0.356081	0.0662	0.185913	0.228809	0.0764	0.333902	0.512723	0.0586	0.11429
A	15:13	15:18	0.05	0.2387434	0.1126	0.471636	0.600633	0.1084	0.180476	0.385953	0.1246	0.322837	0.864855	0.0972	0.11238
A	15:01	15:06	0.05	0.2416256	0.1127	0.466424	0.607884	0.1106	0.181943	0.390612	0.1256	0.321547	0.875296	0.0985	0.11253
A	17:01	17:06	0.1	0.4286054	0.201	0.468963	1.07829	0.1878	0.174165	0.692884	0.2155	0.311019	1.552636	0.172	0.11077
A	16:49	16:54	0.1	0.4337796	0.203	0.46798	1.091307	0.1892	0.17337	0.701249	0.218	0.310874	1.57138	0.178	0.11327
A	15:49	15:54	0.1	0.4606031	0.2168	0.470687	1.15879	0.2055	0.17734	0.744611	0.232	0.311572	1.668548	0.1825	0.10937
A	14:49	14:54	0.1	0.4890852	0.2279	0.465972	1.230446	0.218	0.177172	0.790655	0.243	0.30734	1.771726	0.1938	0.10938
A	14:38	14:42	0.1	0.4944948	0.2357	0.476648	1.244055	0.225	0.18086	0.799401	0.246	0.307731	1.791322	0.199	0.11109
A	14:27	14:30	0.1	0.4999643	0.2234	0.446832	1.257815	0.2315	0.184049	0.808243	0.25	0.309313	1.811135	0.205	0.11318
A	16:01	16:06	0.3	1.3653266	0.5811	0.425612	3.434903	0.554	0.161285	2.207188	0.6065	0.274784	4.945936	0.499	0.10089
A	16:13	16:18	1	4.496802	1.494	0.332236	11.3131	1.445	0.127728	7.269534	1.555	0.213906	16.2898	1.34	0.0822
A	16:25	16:30	2.5	11.107907	2.345	0.211111	27.94539	2.33	0.083377	17.95705	2.5	0.139221	40.23872	2.175	0.05405
A	16:37	16:42	10	43.87969	5.79	0.131952	110.393	5.67	0.051362	70.93594	6.205	0.087473	158.9555	5.495	0.03456
B	15:31	15:36	0.01	0.0468969	0.0224	0.477644	0,117984	0.0214	0.181381	0.075814	0.0242	0.319204	0.169885	0.0195	0.11478
B	15:19	15:24	0.03	0.1423892	0.0654	0.459305	0.358224	0.0628	0.175309	0.230186	0.0727	0.315831	0.515809	0.0568	0.11011
B	15:07	15:12	0.05	0.2401802	0.1104	0.459655	0.604248	0.1038	0.171784	0.388276	0.1198	0.308544	0.87006	0.094	0.10803
B	14:55	15:00	0.05	0.2430797	0.1148	0.472273	0.611542	0.1071	0.175131	0.392963	0.1229	0.312752	0.880564	0.0978	0.11106
B	16:55	17:00	0.1	0.4309692	0.1975	0.458269	1.084237	0.1802	0.1662	0.696705	0.2158	0.309744	1.561199	0.1678	0.10748
B	15:43	15:48	0.1	0.4631434	0.2066	0.446082	1.165181	0.1965	0.168643	0.748718	0.227	0.303185	1.677751	0.1818	0.10835
B	14:43	14:48	0.1	0.4920285	0.223	0.453226	1.23785	0.2105	0.170053	0.795414	0.238	0.299215	1.782388	0.1925	0.10800
B	14:32	14:36	0.1	0.4974707	0.232	0.466359	1.251542	0.218	0.174185	0.804212	0.242	0.300916	1.802102	0.1985	0.11014
B	14:20	14:24	0.1	0.5034763	0.2314	0.459605	1.266651	0.2245	0.177239	0.81392	0.2415	0.296712	1.823858	0.2025	0.11102
B	15:55	16:00	0.3	1.3735432	0.5544	0.403628	3.455574	0.509	0.147298	2.220471	0.57	0.256702	4.975701	0.473	0.09506
B	16:07	16:12	1	4.5238639	1.461	0.322954	11.38118	1.38	0.121253	7.313282	1.495	0.204423	16.38783	1.29	0.07871
B	16:19	16:24	2.5	11.174755	2.329	0.208416	28.11356	2.23	0.079321	18.06512	2.395	0.132576	40.48088	2.1	0.05187
B	16:32	16:36	10	44.099638	5.645	0.128006	110.9463	5.635	0.05079	71.29151	6.165	0.086476	159.7522	5.48	0.03430

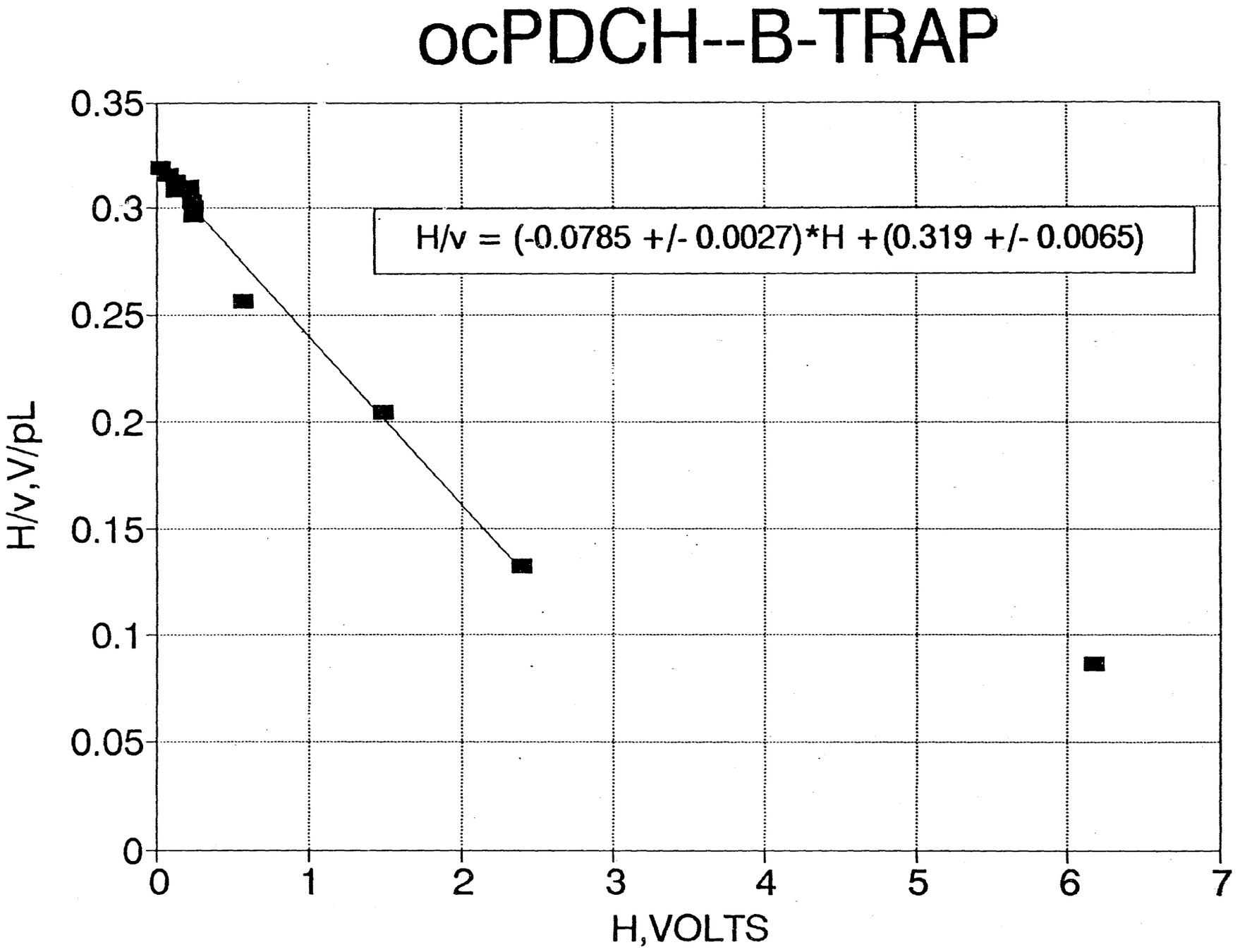

Figure 6. DTA calibration curve for ocPDCH on Trap B.

In use, the height of an unknown peak is divided by the H/v corresponding to that height, to obtain the quantity of tracer which, divided by the sample volume, gives concentration.

The calibration of the laboratory chromatograph system is beyond the scope of this report and is described in detail elsewhere.(3)

TRACER SOURCE ANALYSES

The two primary tracers used in this study were the leaking tracer, ocPDCH, prepared as a standard in a small cylinder for filling the surrogate-module at the test site and the reference tracers, pt PDCH and PMCP. For this study, the ptPDCH was selected as the reference to work up the data primarily because it is better resolved on the DTA than is PMCP.

Leaking Tracer Analysis

The PFT composition of the surrogate-module leaking tracer was analyzed both on the DTA and the laboratory GC system. The response to the analysis of three consecutive samples on the DTA is shown in Figure 7. The comparison of the expected PFT concentrations versus that obtained from the laboratory GC is

	Concentration, µL/L (ppm)		
	PMCH	ocPDCH	ptPDCH
Laboratory GC:	0.476	4.27	0.0488
Expected:	0.216	4.18	0.0369

The laboratory GC analysis results were used in all calculations rather than the expected composition based on the dilution from a 10-fold higher concentration standard since its analysis was uncertain. However, the agreement for ocPDCH was excellent in any regard. There was a significant discrepancy only for the PMCH which could have served as an alternative reference tracer but was not evaluated in this study; it was present at about 11.1% of the ocPDCH. Note also that ptPDCH, the reference tracer, was present at about 1.14% of the ocPDCH. Since the reference tracer concentration in the building air was always much higher than that of the leaking tracer, no correction was necessary.

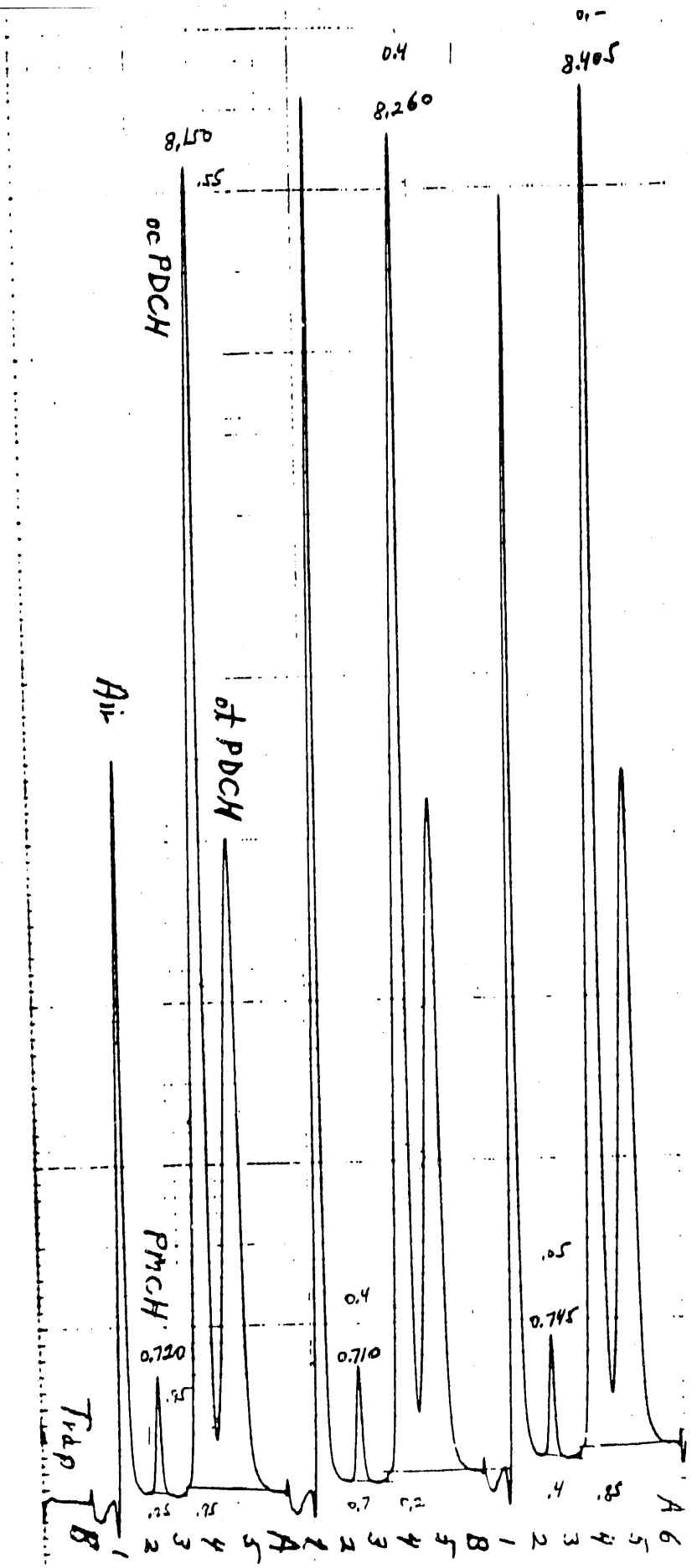

Figure 7. Lab analysis of leaking tracer on DTA showing PMCH, ocPDCH, and otPDCH.

Reference Tracer Compositions and Source Rate

The pure tracers used to make the reference tracer permeation sources were previously analyzed to have the following composition:

	Concentration, % by volume			
PFT Source Type	PMCP	PMCH	ocPDCH	ptPDCH
PMCP	89.0	---	---	---
pPDCH	---	---	0.15	55.04

The balance of the above compositions included isomers and other components not of interest.

Since the ratio of oc/pt in the pPDCH was 0.00273, a correction was applied to the ocPDCH measurement data to account for the small amount coming from the reference tracer rather than just the "leak" from the surrogate-module tracer source.

The source rates for the reference PFTs were

			Rate at 22°C	
Type	Code	Quantity	nL/min for 1	S_r, nL/h @ qty
PMCP	8I	1	32.8	1968 ± 157
ptPDCH	5F	10	8.25	4950 ± 396

A temperature of 22°C in the building was assumed throughout the late morning and early afternoon for this study. The rate at other temperatures can be computed by assuming a $\Delta H/R$ of 3400 cal/mole, if desired. That activation energy gives a response of S_r to a temperature change equivalent to 4%/°C; thus, a temperature uncertainty of ±2°C gives an S_r uncertainty of ±8%.

DTA AND BATS ANALYSES

The analysis results and the derivative fit of the data to Eq. (4) in order to compute leak rates are shown in Table 2 for the DTA and Tables 3 and 4 for the two BATS units. The ocPDCH concentrations shown have been corrected for the contribution from the reference tracer, which contained 1.14% of the ptPDCH as ocPDCH. A discussion of the derivative fit results is presented later; this section only presents the analytical results and discussion of related observations.

Table 2. DTA analysis and derivative fit leak rate results.

TRAP	TIME ANAL-3min	SAMPLE VOLUME (L)	PMCP	PMCH	ocPDCH	ptPDCH	oc/pt	dC/dt (ocPDCH)	dC/dt (ptPDCH)	(oc/pt) *Sr(pt)	dC/dt(pt) *oc/pt *VOL	dC/dt(oc) *VOL	nL(oc) /min	Leak (ml/min)
			picoliters/liter											
B	10:40	1.24			0.00431	0.274228	0.015716	0.00033	-0.00103	1.296543	-0.07495	1.532648	2.904144	0.680127
A	10:46	1.24	0.06324	0.005643	0.006829	0.231938	0.029443	-3.1E-05	-0.00422	2.429066	-0.57792	-0.14251	2.864476	0.670837
B	10:52	1.24		0.001801	0.003942	0.223574	0.017631	-0.00035	-0.00211	1.454584	-0.17322	-1.62601	0.001786	0.000418
A	10:58	1.24	0.062875	0.007524	0.002633	0.206584	0.012745	-0.00018	-0.00024	1.051425	-0.01427	-0.82482	0.240868	0.056409
B	11:04	1.24			0.00142	0.220685	0.006436	0.001195	0.003074	0.530944	0.092001	5.556473	5.995416	1.404079
A	11:10	1.24	0.068348	0.002351	0.006797	0.243476	0.027919	0.00071	0.002772	2.303278	0.359814	3.299443	5.242907	1.227847
B	11:16	1.24		0.001801	0.009935	0.253944	0.039123	0.000358	-0.0009	3.227612	-0.16326	1.665548	5.056425	1.184174
A	11:22	1.24	0.065063	0.00188	0.011096	0.232706	0.047681	-3.2E-05	-0.00379	3.933682	-0.84125	-0.14814	4.626788	1.083557
B	11:28	1.24		0.001351	0.009553	0.208413	0.045835	-0.00021	-0.00038	3.781398	-0.08193	-0.97224	2.891094	0.677071
A	11:34	1.24	0.06853	0.007524	0.033575	0.228093	0.147201	0.002893	0.002227	12.14405	1.524262	13.45196	24.07175	5.637413
B	11:40	1.24		0.001801	0.046594	0.235136	0.198156	0.002917	-0.00141	16.34786	-1.29787	13.56392	31.20965	7.309051
A	11:46	1.24	0.066888	0.008936	0.068579	0.211191	0.324726	0.002649	-0.00448	26.78989	-6.76316	12.31942	45.87247	10.74297
B	11:52	10.88		0.01083	0.078386	0.181388	0.432143	0.001329	-0.00404	35.65182	-8.11491	6.178832	49.94556	11.69685
A	11:58	12.81	0.009384	0.002643	0.02433	0.078679	0.309227							
B	12:04	2.05		0.003541	0.076017	0.222187	0.342129	-0.00054	0.008153	28.22565	12.97031	-2.52057	12.73477	2.982382
A	12:10	1.24	0.060142	0.010818	0.073577	0.258874	0.28422	-0.00201	0.000558	23.44815	0.737089	-9.34805	13.36302	3.129513
B	12:16	1.58		0.003534	0.051893	0.228879	0.226725	-0.00236	0.001413	18.70478	1.489738	-10.9763	6.238779	1.461072
A	12:22	1.24	0.064699	0.099236	0.045251	0.275831	0.164055	-0.00144	0.002149	13.53454	1.639425	-6.71506	5.180052	1.213127
B	12:28	1.24		0.001351	0.034563	0.254668	0.135719	-0.00145	0.001157	11.19684	0.730384	-6.73436	3.7321	0.874028
A	12:34	1.24	0.079501	0.008465	0.036893	0.289719	0.12734	-0.00176	-0.00042	10.50554	-0.25	-8.17592	2.579618	0.604126
B	12:40	1.24		0.002701	0.028981	0.249602	0.116107	-0.00107	-0.00379	9.578861	-2.04592	-4.98532	6.639465	1.55491
A	12:46	1.24	0.064152	0.017409	0.155518	0.244245	0.63673	0.017028	-0.00036	52.53019	-1.07114	79.18143	132.7828	31.09666
B	12:52	1.24		0.018475	0.23332	0.24526	0.951315	0.010542	0.000137	78.4835	0.608233	49.02123	126.8965	29.71815
A	12:58	1.24	0.06324											
B	13:04	1.24		0.393219										
A	13:10	1.24	0.048141	0.243796										
B	13:16	1.24		0.247769	2.004154	0.214909	9.32561	0.13265	0.02717	769.3628	1178.212	616.8237	207.9741	48.70588
A	13:22	1.24	0.109845	0.192326	1.591803	0.326043	4.88219	-0.1301	-0.01791	402.7807	-406.575	-604.942	204.4129	47.87188
B	13:28	1.24		0.042865	0.443012									
A	13:34	1.24		0.008465	0.10071	0.0379	2.657281	-0.00669	0.004154	219.2256	51.33138	-31.0884	136.8058	32.03883
B	13:40	1.24		0.004503	0.070624	0.049851	1.416704	-0.00595	-0.00063	116.8781	-4.16543	-27.6739	93.3696	21.86642
A	13:46	1.24			0.029293	0.030312	0.96639	-0.00395	-0.00178	79.72716	-8.00873	-18.3645	69.3714	16.24623
B	13:52	1.24		0.001351	0.023232	0.028464	0.81617	-0.0003	0.002404	67.33404	9.125484	-1.37907	56.82949	13.30901
A	13:58	1.24			0.025734	0.059166	0.434951	0.000339	0.002734	35.88349	5.529249	1.576675	31.93092	7.477966
B	14:04	1.24			0.029749	0.061271	0.485535	0.035064	0.003361	40.05664	7.589284	163.0456	195.5129	45.78757
A	14:10	1.24		0.018822	0.187535	0.099503	1.884714	0.026509	0.003217	155.4889	28.19784	123.2685	250.5596	58.67907
B	14:16	1.24		0.0397	0.347861	0.09988	3.482778	0.034257	0.006303	287.3292	102.0845	159.2943	344.5389	80.68828
A	14:22	1.24	0.047052	0.063675	0.598617	0.175145	3.417836	0.018634	0.004903	281.9714	77.92058	86.64879	290.6996	68.07954
B	14:28	1.24		0.06324	0.571471	0.158715	3.600622	-0.00452	0.001597	297.0513	26.73624	-21.0381	249.277	58.37869
A	14:34	1.24	0.051955	0.077883	0.738406	0.194308	3.800191	0.005484	0.004683	313.5158	82.74989	25.50075	256.2667	60.01561
B	14:40	1.24		0.085024	0.77131	0.214909	3.589014	0.004459	0.000222	296.0937	3.710276	20.73232	313.1157	73.3292

Table 3. BATS (near DTA) analysis and derivative fit leak rate results.

FILE	CLOCK HRS	FEMTOLITERS/LITER PMCH	ocPDCH	ptPDCH	PMCP	RATIO oc/pt	dC/dt (ocPDCH	dC/dt (ptPDCH	Rv(t) (ptPDCH	(oc/pt)* Sr(pt)	dC/dt(pt) *oc/pt *VOL	dC/dt(oc) *VOL	nL(oc)/ min	Leak (ml/min)
7337B1	9.125	3.61	0.24	15.39	12.67	0.015799								
7337B2	9.375	4.82	1.67	13.38	7.32	0.12512	0.000166	0.001963	10027.02	10.32244	1.141817	0.770585	9.951206	2.330493
7337B3	9.625	4.68	5.21	74.26	50.80	0.070218	0.000108	0.005531	1117.725	5.792961	1.805859	0.504316	4.491418	1.051854
7337B4	9.875	5.35	4.93	179.30	142.55	0.027483	-6E-05	0.006369	370.9683	2.267382	0.813981	-0.27973	1.173671	0.274864
7337B5	10.125	5.75	3.41	265.34	193.07	0.012851	-4.7E-05	0.003327	347.1618	1.060211	0.198835	-0.21902	0.642359	0.150435
7337B6	10.375	6.42	3.51	279.12	196.73	0.012592	1.28E-05	0.000526	406.9116	1.038877	0.030818	0.05961	1.067669	0.250039
7337B7	10.625	4.82	3.79	281.13	196.87	0.013497	-3.3E-05	-6.7E-05	420.6322	1.113523	-0.0042	-0.15383	0.963892	0.225736
7337B8	10.875	8.56	2.52	277.12	212.92	0.009102	-6.9E-05	0.000105	385.1912	0.750939	0.004431	-0.32061	0.425897	0.099742
7337B9	11.083	6.42	5.00	284.01	258.79	0.0176	0.000681	0.000485	310.0805	1.451965	0.039666	3.16886	4.58116	1.072871
7337B10	11.25	7.63	10.12	288.02	244.02	0.035135	0.000458	0.000511	328.3507	2.898647	0.083528	2.129062	4.944181	1.157888
7337B11	11.4167	13.45	14.17	294.24	248.45	0.048143	0.000329	0.000573	321.344	3.971776	0.128185	1.529295	5.372886	1.258287
7337B12	11.583	13.65	39.17	299.46	267.02	0.130805	0.004759	-0.00063	319.9722	10.79138	-0.3846	22.12734	33.30332	7.799372
7337B13	11.75	24.49	74.93	281.60	263.65	0.266093	0.003781	-3E-05	313.4494	21.95268	-0.03721	17.58144	39.57133	9.267291
7337B14	11.9167	21.28	114.87	298.86	275.68	0.38437	0.003247	0.000412	292.3144	31.71056	0.73615	15.09686	46.07127	10.78952
7337B15	12.083	16.66	103.78	289.83	277.37	0.358067	-0.0045	1E-05	297.2714	29.54052	0.016711	-20.9219	8.601906	2.014498
7337B16	12.25	23.88	69.97	299.06	291.51	0.233951	-0.00276	0.001474	259.5029	19.30093	1.603106	-12.832	4.865807	1.139533
7337B17	12.4167	30.91	48.53	319.33	311.35	0.15196	-0.00174	0.00218	232.4167	12.53672	1.54036	-8.10363	2.892728	0.677454
7337B18	12.583	35.33	34.78	342.62	319.58	0.101503	0.009964	0.000512	250.7	8.373973	0.241596	46.33347	54.46584	12.75547
7337B19	12.75	34.72	109.66	329.57	330.14	0.332728	0.595119	0.005985	165.6006	27.45008	9.259437	2767.301	2785.492	652.34
7337B20	12.9167	1176.18	11950.24	462.44	226.50	25.84158	0.287015	0.001698	329.3912	2131.93	204.0038	1334.618	3262.544	764.0618
7337B21	13.083	599.13	5844.21	363.49	252.88	16.078	-0.42471	-0.00659	447.4926	1326.435	-492.991	-1974.89	-155.462	-36.4079
7337B22	13.25	384.97	3456.95	330.57	246.55	10.45741	-0.1937	-0.00267	384.9925	862.7363	-129.874	-900.699	91.91143	21.52492
7337B23	13.4167	224.47	1756.14	291.44	225.44									

Table 4. BATS (opposite DTA) analysis and derivative fit leak rate results.

FILE	CLOCK HRS	FEMTOLITERS/LITER PMCH	ocPDCH	ptPDCH	PMCP	RATIO oc/pt	dC/dt (ocPDCH	dC/dt (ptPDCH	Rv(t) (ptPDCH	(oc/pt)* Sr(pt)	dC/dt(pt) *oc/pt *VOL	dC/dt(oc) *VOL	nL(oc)/ min	Leak (ml/min)
7338B1	9.375	9.99	0.85	23.37	19.03	0.036425								
7338B2	9.625	12.49	5.93	126.86	92.66	0.046728	0.000109	0.008119	352.6939	3.85509	1.764261	0.50477	2.5956	0.607869
7338B3	9.875	11.49	4.11	266.95	125.08	0.015388	-8.4E-05	0.006656	193.108	1.269484	0.476232	-0.38841	0.40484	0.09481
7338B4	10.125	14.87	3.42	326.53	154.09	0.010481	-5.8E-05	0.003809	198.4061	0.864651	0.185649	-0.27123	0.407768	0.095496
7338B5	10.375	6.87	2.36	381.24	178.24	0.006185	-4.4E-05	0.001746	195.1016	0.510258	0.050224	-0.20452	0.255512	0.059839
7338B6	10.625	6.12	2.10	378.92	148.71	0.005549	-1.4E-05	0.000158	215.7783	0.457823	0.004087	-0.06279	0.390942	0.091556
7338B7	10.875	5.12	1.95	385.99	165.77	0.005059	-8.1E-06	0.002248	186.6616	0.417386	0.052875	-0.0378	0.326707	0.076512
7338B8	11.083	3.75	8.21	440.69	211.84	0.018627	0.000587	0.000873	177.9944	1.536729	0.075629	2.728387	4.189487	0.981144
7338B9	11.25	4.31	12.62	405.63	172.86	0.031107	0.000603	0.001626	184.7492	2.566349	0.235163	2.802727	5.133913	1.202322
7338B10	11.4167	5.25	20.28	473.24	157.70	0.042847	0.000623	0.00213	153.3973	3.534854	0.424465	2.894736	6.005125	1.406352
7338B11	11.583	9.56	70.35	448.20	188.21	0.156951	0.003753	-0.00421	227.7369	12.94842	-3.07174	17.4495	33.46966	7.838328
7338B12	11.75	12.37	98.55	389.07	162.03	0.253286	0.004038	-0.00124	226.8765	20.89613	-1.46158	18.77747	41.13517	9.63353
7338B13	11.9167	16.49	151.20	423.35	143.92	0.357143	0.00428	0.002535	167.0256	29.46427	4.210457	19.90086	45.15466	10.57486
7338B14	12.083	11.81	114.49	439.72	124.43	0.260358	-0.00503	0.003236	153.3961	21.47956	3.917883	-23.3763	-5.81457	-1.36173
7338B15	12.25	8.62	76.71	488.07	136.04	0.157164	-0.00317	0.003502	135.6725	12.96602	2.559022	-14.7533	-4.34627	-1.01786
7338B16	12.4167	6.00	50.96	509.83	127.18	0.099956	-0.00209	-0.00176	177.9075	8.2464	-0.81996	-9.73118	-0.65482	-0.1557
7338B17	12.583	4.87	35.82	452.82	108.28	0.07911	0.028132	-0.00352	218.291	6.52656	-1.29319	130.8119	138.6316	32.46642
7338B18	12.75	27.36	247.23	439.53	98.83	0.562489	0.055308	-0.00229	211.9217	46.40531	-5.9884	257.183	309.5767	72.50039
7338B19	12.9167	130.99	1143.20	406.98	89.58	2.808985	0.261866	0.001244	188.5038	231.7412	16.24317	1217.678	1433.176	335.6385
7338B20	13.083	558.08	5479.32	464.38	92.53	11.79927	0.119173	0.001984	157.7898	973.4398	108.8587	554.1552	1418.736	332.2567
7338B21	13.25	389.61	3526.43	446.66	82.89	7.895141	-0.18574	-0.00681	255.6103	651.3491	-250.042	-863.681	37.71008	8.8314
7338B22	13.4167	229.19	1760.48	328.01	54.53	5.367121	-0.17209	-0.01944	527.1597	442.7875	-485.265	-800.217	127.8357	29.93811
7338B23	13.583	20.24	88.08	58.17	0.00	1.514184	-0.13627	-0.02199	3175.978	124.9202	-154.809	-633.643	-353.914	-88.4785

DTA Analyses

The results in Table 2 are grouped according to the particular period--just before the first run, then run numbers 1, 2, and 3, then the overdosing of ocPDCH period from about 1246 through the building air purge period, the period just before run no. 4, and then run no. 4 from 1404 to about 1440. The first column shows which trap the sample was collected on for the 6-min cycle and the next column is the mid-time for the collection period which is equivalent to the start of the analysis minus 3 min. The sample volume was usually 1.24 L except for the few samples near the end of run no. 2 (1152 to 1158) when the higher pumping rate was tested.

The concentration found for the four tracers are shown next. The chromatograms of the 5 samples collected during run no. 1 (1104 to 1128) are shown in Figure 8 and the 4 for run no. 2 (1134 to 1158), Figure 9. The small ocPDCH concentration of 0.00142 pL/L measured for the 1104 sample is reflected in the small peak, so labelled, for the chromatogram in Figure 8. By the next chromatogram, the ocPDCH peak at the 4-min location has clearly grown as it has by the next analysis of the 1116 sample. The peak heights, in inches, are marked just above the peaks; the increasing concentration is reflected by the data in Table 2.

For run no. 2, the first analysis (the 1134 sample in Figure 9) clearly shows the rapid increase in the ocPDCH peak. The sample at 1152 shows a substantial increase in the size of the peak (a height increase of 5.13/1.29 = 4.0 times a gain reduction of 2.5 gave a 10-fold increase) because the sample volume was increased about 10-fold for that and the subsequent run (trap A was not as efficient as trap B at the higher sampling rate).

Clearly, even from the chromatograms without any further analysis, leak rates in the range of the 0-10 mL/min transducer were readily apparent in less than one-half hour.

BATS Analyses

The results of the two BATS unit analyses are displayed in Tables 3 and 4 in a similar way to the DTA results. The BATS were analyzed on the laboratory GC system at Brookhaven which is a completely automated system including a PE Nelson data acquisition and integration system which

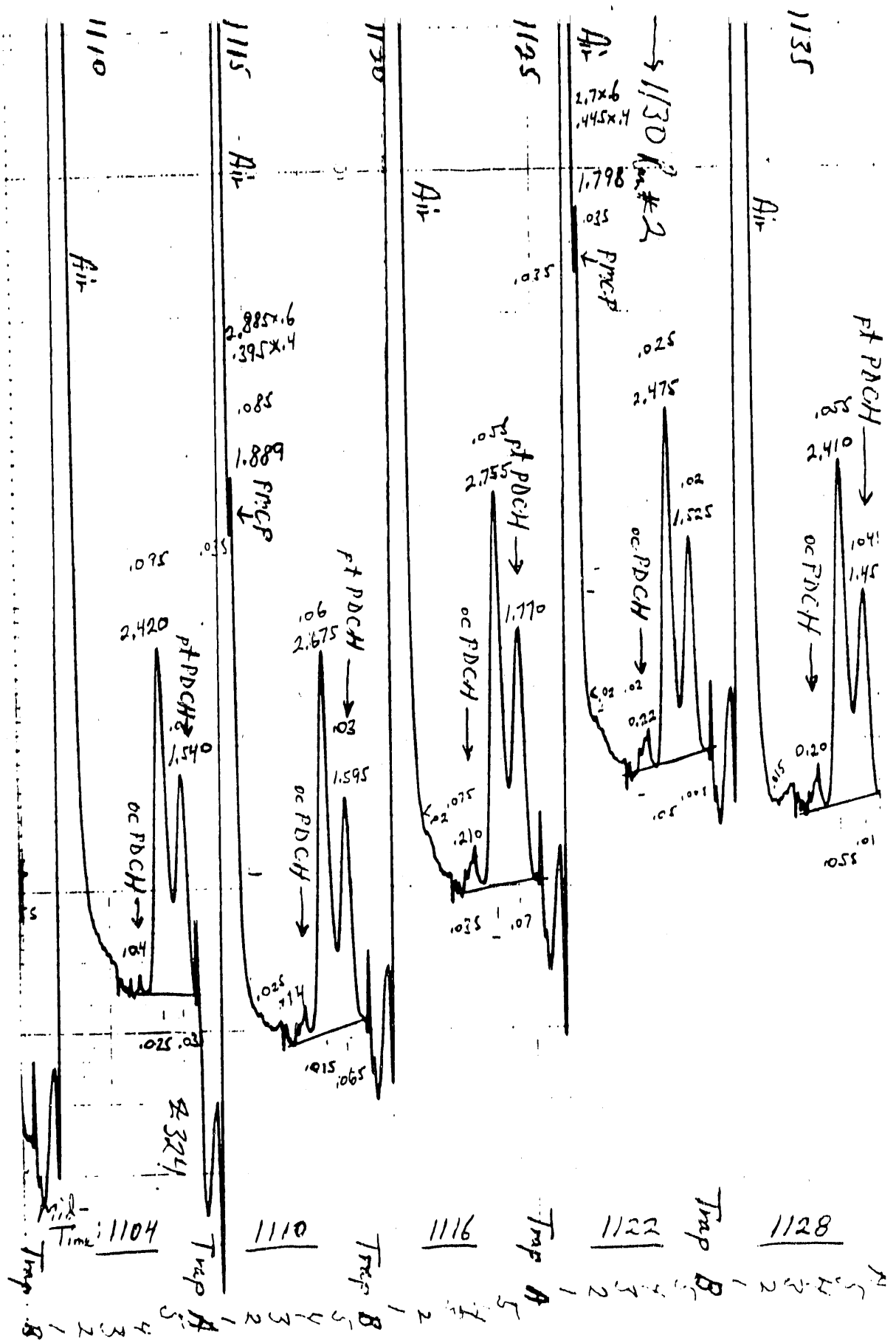

Figure 8. DTA chromatograms from the run no. 1 period.

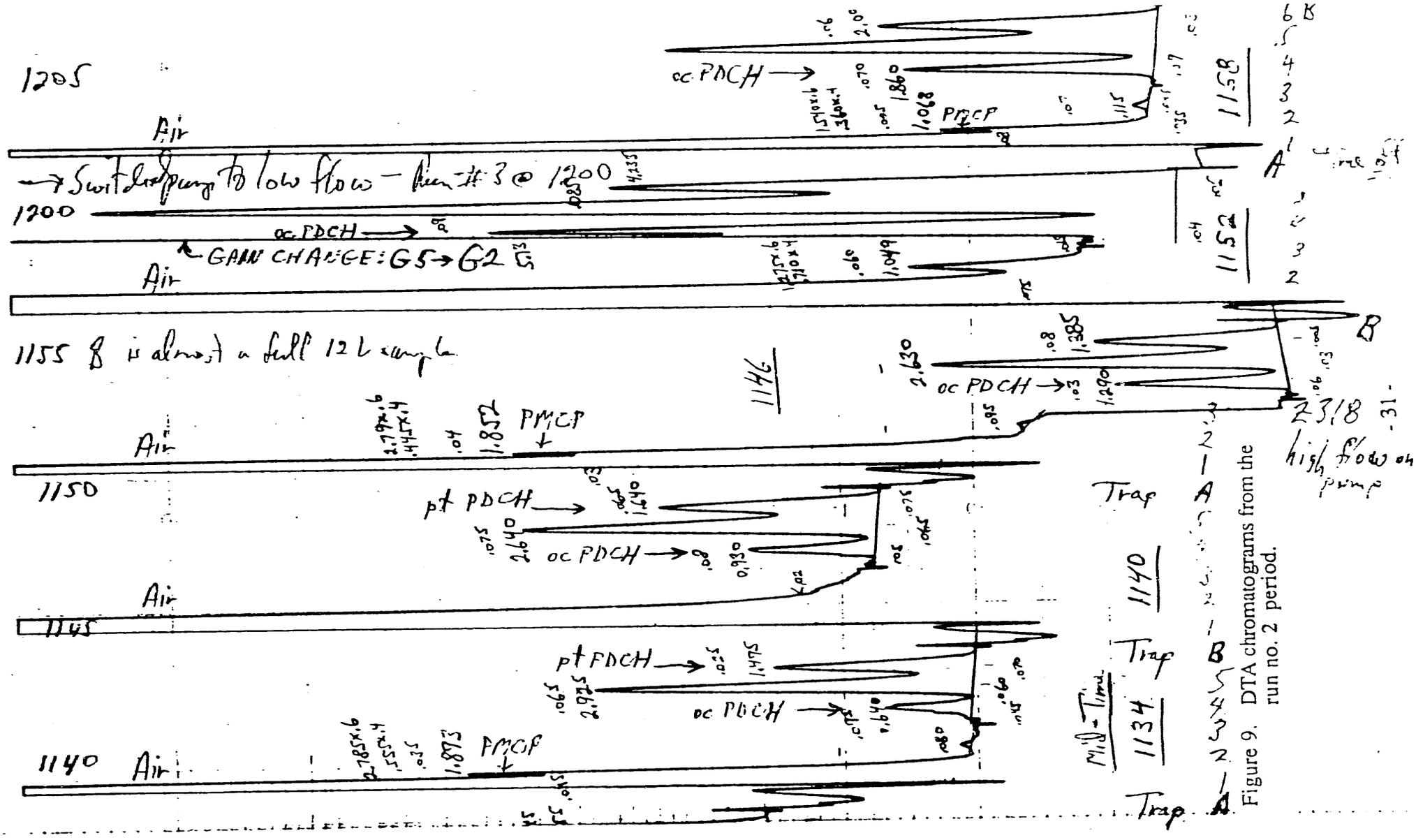

Figure 9. DTA chromatograms from the run no. 2 period.

greatly enhances both the resolution of the different PFTs and the limits of detection. Examples of the chromatograms from run nos. 1 and 2 and a demonstration of the systems ultimate detection capability, available from these results, is given in Appendix A. It is this system that Brookhaven is proposing to build for NASA for the future certification of all SSF modules.[8]

The first column in Tables 3 and 4 gives the computerized data system file number for each sample analysis, a total of 23 for each BATS which is the total number of tubes in each lid assembly. The next column is the mid-time in hours of the collected samples, which were 15 minutes in duration until 1100, the start of the first run, and of 10-min duration thereafter. The next four columns are the 4 PFT analyses results followed by the oc-to-pt PDCH ratio, C'_ℓ ,which is used to portray the results in Figures 1 to 4 as well as to calculate the leak rates.

BATS near DTA (File 7337B). The first sample collected from 0900 to 0915 and the second from 0915 to 0930 should have had ambient PFT levels since no tracer was in the building at the time. Indeed, the PMCH and ocPDCH in the first sample are at ambient (3.5 and 0.25 fL/L, respectively) but the ptPDCH and the PMCP (the reference tracers used in this test) are both about 3 to 4 times their ambient background levels, implying that some of their vapors got into the building either because the car containing the sources was parked just outside on the upwind side of the building, because the car's occupants carried PFT-laden air into the building (in lungs, etc.--probably unlikely), or the sources were brought into the building briefly and then back outside before 0900. The first case would require about 3.7% of the total PFT source strength in the car to be entering the building; the second case would require about 17L of air from the car to be brought into the building; the last case would require that the sources were inadvertently brought into the building for about 1 min.

By the third sample, the ocPDCH level climbed more than 10-fold. But the surrogate module filled with the ocPDCH standard was not brought into the building until 1030. The only explanation is that a small amount of the module tagging gas was leaking in from outside during the filling operation. That this can occur is demonstrated by the 300-fold increase in the ocPDCH building concentration at 12.9 hours because the surrogate module was vented just outside. These observations point out both the sensitivity of the PFT technology and the care that must be exercised in its use.

BATS opposite DTA (File 7338B). The first sample collected with this unit was from 0915 to 0930, 15 min after the start of the other BATS. For the same time intervals, the ocPDCH values track each other on both samples, although the magnitudes are slightly different because of their different physical locations in the building; thus the building was not a perfectly well-mixed single zone.

On this sampler, remembering that the module tagging gas contained about one-tenth as much PMCH as ocPDCH, the PMCH tracks the ocPDCH quite well, increasing in runs 1 and 2 when the ocPDCH increases and decreases, as does the ocPDCH in run number 3. There was occasionally some deviation of this phenomenon on the sampler near the DTA, because there was some interference with the PMCP and PMCH analyses on that sampler.

Similarly, there were two reference tracers, ptPDCH and PMCP, with an emission rate ratio of 2.52 to 1. On this sampler, there ratio as analyzed, excluding the first two samples, was 2.42 ± 0.32 through the noon time sample. After that, the ratio increased because of interference with the PMCP analysis; on the first BATS unit this ratio was also poor because of PMCP interference (the analyses results reported are too high). No interference was seen on either sampler for the leaking tracer, ocPDCH, or the reference tracer, ptPDCH; thus, they were the tracers of choice for the determination of leak rates.

BUILDING VOLUME (V_B) AND AIR TURNOVER TIME (τ)

As shown in the theory section on leak quantification, the volume of the building, V_B, is needed for the derivative solution of Eq. (4) and the time for one complete change of air in the building, τ, is needed for the integral solution.

Applying Eq. (19) to the ptPDCH reference tracer results of Files 7338B2 to 7 (samples collected between 0930, when the source was brought into the building, and 1100) and plotting the adjusted concentration over time versus time as shown in Fig. 10, gave an excellent linear regression result

$$\text{Adjusted } \frac{C_r(t)}{t} = a - bt$$

$$a = 1.0902 \pm 0.0098$$

$$b = 1.4755 \pm 0.0114$$

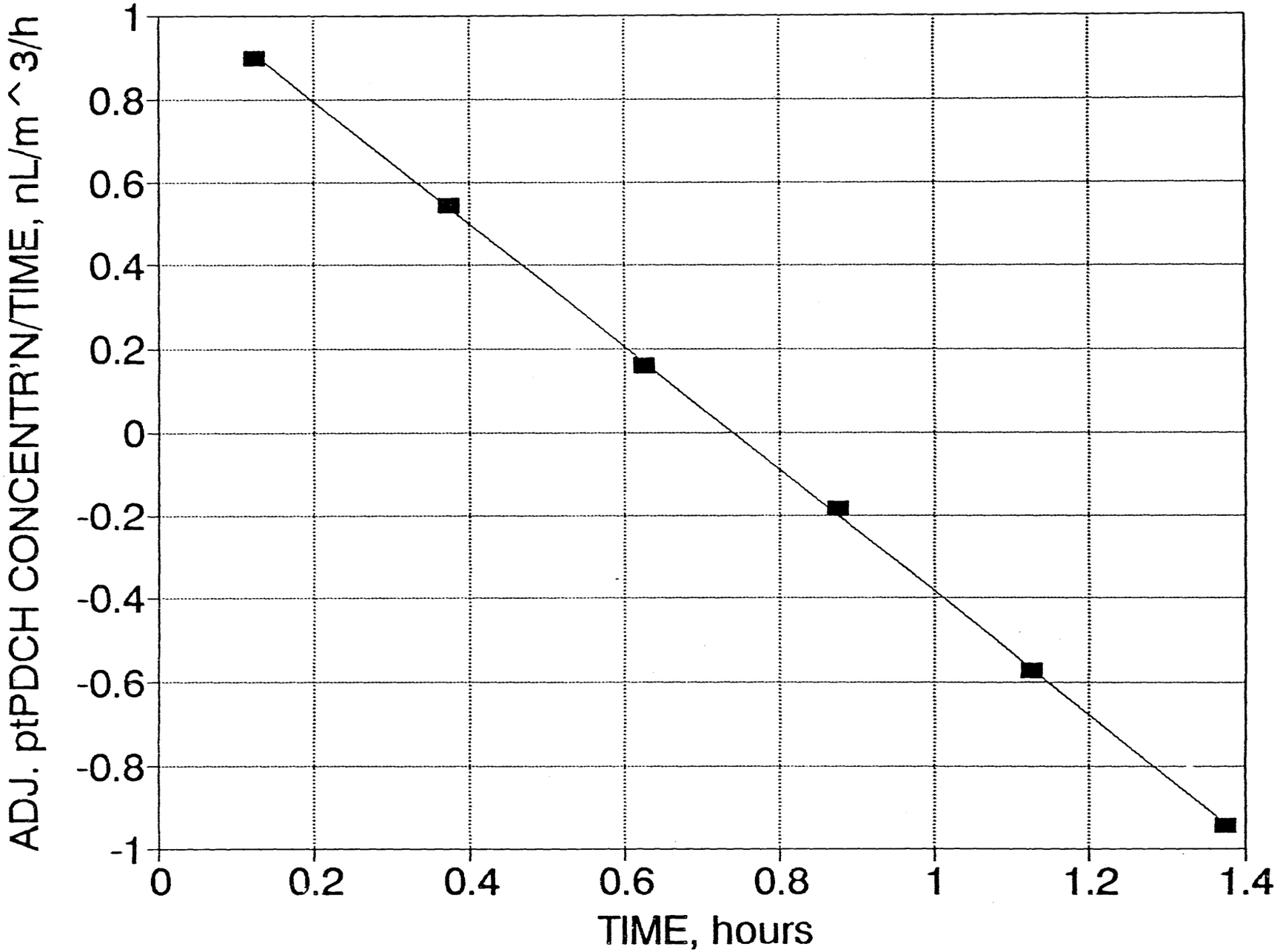

Figure 10. BATS data from unit across the room from the DTA. (Determination of V_B and τ).

with an r^2 of 0.999976. This good fit implied that the location across the room from the DTA was a representative sampling point for this leak quantification study as well as for assessing the air flow performance of the building.

This volume of the building is, from Eq. (17),

$$V_B = \frac{S_r}{a} = \frac{4950 \pm 396}{1.0902 \pm 0.0098} = 4541 \pm 366 \text{ m}^3$$

and the air turnover time is, from Eq. (18),

$$\tau = \frac{a}{2b} = 0.3694 \pm 0.0044 \text{ h}$$

The volume of the building is, or course, independent of time and the above value can be used in Eq. (4) for calculating S_ℓ for all measurements.

On the other hand, as determined above, τ is the average turnover time for the period from 0930 to 1100 and may, of course, be variable with time. The integral solution given by Eq. (14) requires an estimate of an average τ for each of the runs. From Eq. (2) at steady state

$$R_E = S_r/C_r$$

and from Eq. (17)

$$V_B = \frac{S_r}{a}$$

where a is a constant value for all times since V_B and S_r are constant. Substituting into the definition of the air turnover time

$$\tau = V_B/R_E$$

gives

$$\tau = \frac{S_r}{a} \bullet \frac{C_r}{S_r} = \frac{C_r}{a}$$

for each measurement period and

$$\bar{\tau} = \frac{\bar{C}_r}{a} \qquad (20)$$

where $\bar{\tau}$ and $\bar{C}_r$ are the average τ and average C_r for each run period, respectively. The values computed from the average of the ptPDCH reference tracer concentrations in Table 4 and substituted into Eq. (20) for each of the run periods are

Time Period	$\bar{C}_r$(pt PDCH)), nL/m^3	$\bar{\tau}$, h
0930 - 1100	0.403± 0.006[a]	0.369 ± 0.004
1015 - 1100	0.382 ± 0.004	0.350 ± 0.005
1100 - 1130	0.440 ± 0.034	0.404 ± 0.031
1130 - 1200	0.420 ± 0.030	0.385 ± 0.028
1200 - 1230	0.479 ± 0.036	0.439 ± 0.033
1405 - 1443	0.401 ± 0.006[b]	0.368 ± 0.010

[a] Computed from Eq. (20), $\bar{C}_r = a\bar{\tau}$

[b] Adjusted for the 1.14% of ocPDCH as pt PDCH.

The above values of τ are then used in the integral solution for S_ℓ, for each run period, given by Eq. (14).

Equation (19) was also applied to the PMCP reference tracer results of Files 7338B3 to 7 excluding B6, which was low, giving

$$a = 0.4518 \pm 0.0114$$

$$b = 0.6310 \pm 0.0206$$

which gave

$$V_B = \frac{1968 \pm 157}{0.4518 \pm 0.0114} = 4356 \pm 364 \text{ m}^3$$

and

$$\tau = \frac{a}{2b} = 0.3580 \pm 0.0148 \text{ h}$$

close to the values of V_B and τ determined from the ptPDCH reference tracer. Thus, the best estimate of the effective volume of the building is

$$V_B = 4450 \pm 260 \text{ m}^3$$

A similar attempt to use the BATS data from the unit near the DTA (File 7337B) would not result in a linear fit to Eq. (19). The average reference tracer concentration from 1100 to 1230 for the BATS across the room was 0.446 ± 0.030 nL/m^3, whereas for the BATS near the DTA, the average ptPDCH concentration was 0.295 ± 0.007 nL/m^3. This large significant difference was due to a local dilution of all the tracer concentrations near the DTA by local infiltration of outside air at that location. Thus, the ratio of oc to ptPDCH was not affected by this dilution and the proper time constant, τ, at that location was the same values used for the BATS across the room, not those attempted to be derived from a biased, non-representative sampling location.

The average ptPDCH concentration from the DTA was 0.237 ± 0.015 nL/m^3, about 20% less than that from the BATS near the DTA. This difference, which did not affect the oc-to-ptPDCH ratio which was the same for both instruments, was partly the result of a change in the efficiency of the DTA traps between the test and the calibration in February. The DTA trap had been contaminated by an overdose of ocPDCH from a leak in the leaking standard cylinder in the same trunk with the DTA during the return shipment. The traps required an extensive bakeout which cleared them of the ocPDCH contamination but also changed (increased) their efficiency. Additionally, there was a question about the absolute magnitude of the standard need to calibrate the DTA but not the relative response between tracers. The absolute magnitude of the laboratory GC system response,which is reflected in the absolute magnitude of τ is known to within ± 5 to $\pm 10\%$.

SURROGATE-MODULE LEAK RATES

The leak rates during the four runs were computed from the two procedures described earlier--the derivative fit and the integral fit to the fundamental leak rate Eq. (4) to obtain S_ℓ followed by substitution in Eq. (5) to calculate the surrogate-module leak rate, R_ℓ. As a review, the information derived in the earlier sections which is needed to solve Eq. (4) for the derivative fit or Eq. (14) for the integral fit is

$$S_r = 4950 \pm 396 \text{ nL/h}$$

$$V_B = 4541 \pm 366 \text{ m}^3$$

The turnover times, t, are specific for each period of the integral fit and are given in the previous section. This section will give the results for the DTA data and the BATS data.

DTA-Determined Leak Rates

The DTA data in Table 2 (see DTA and BATS Analysis Section) was used to calculate the surrogate-module leak rate by both methods. After the column giving the oc/pt ratio are the derivatives for both the ocPDCH and ptPDCH obtained from the appropriate equations--either Eqs. (8), (9), or (10). The next three columns give the computed values for the three terms of Eq. (4) and the next to the last column--nL(oc)/min, is S_ℓ, the rate of the leaking tracer. The time base in these data are minutes. Finally, the last column gives R_ℓ, the module air leakage rate (mL/min).

Because the reference tracer concentration is essentially at steady state, the middle term containing $dC_r(pt)/dt$ should be small compared to the other two terms. Also, the first term, $S_r C_\ell(t)/C_r(t)$, should dominate toward the end of runs 1, 2, and 4, when the leaking tracer concentration is approaching steady state from below. This is generally seen to be the case.

The leak rates shown in the last column, grouped according to the run period, were averaged as shown in Table 5. Also shown is the steady state solution estimate using Eq. (7) on the last two points in each run period and the results of the integral fit solution using Eq. (14). As mentioned earlier, the steady state solution is just an estimate which, in this case, is reasonably good. The integral fit, because it makes use of all the data collected in a single period, should be the more reliable result.

BATS-Determined Leak Rates

The BATS data results are shown in Table 3 and 4. Again, for each run, the middle term of Eq. (4) is small compared to the first and third terms and, as steady state is approached, the first term becomes more significant than the third.

Table 5

Leak Rates from Real-Time Analyzer (DTA) Results

Run No.	Time Period	Steady State	Integral Fit	Derivative Fit
	1037-1101	0.29 ± 0.07	-0.08 ± 0.17	0.35 ± 0.37
1	1101-1131	0.90 ± 0.03	1.35 ± 0.10	1.12 ± 0.27
2	1131-1201	8.35	11.24 ± 2.06	8.85 ± 2.85
3	1201-1231	2.54 ± 0.11	-0.53 ± 0.54	1.93 ± 1.05
	1343-1405	2.10 ± 0.33	1.61 ± 0.37	12.3 ± 4.5
4	1405-1443	63.4 ± 2.0	82.8 ± 7.9	66.5 ± 9.2

The leak rates from the programmable samplers are summarized in Table 6. Because the laboratory GC system is several orders of magnitude more sensitive and precise than the DTA, the agreement between the integral fit- and derivative fit-results is much better.

There is an additional column in the BATS tables, the 6th from the end, labeled $R_V(t)$(ptPDCH), which is actually the exfiltration rate, R_E, computed from Eq. (2). Note that during runs 1 and 2, R_E averages 314 ± 13 m^3/min for the BATS near the DTA and 190 ± 31 m^3/min for the BATS across the room. As mentioned before, the 65% higher exfiltration rate near the DTA site is most likely due to the local dilution of the air at this site by nearby inleakage of outside air; several large vents were located on the upwind wall just behind the DTA site.

This factor of 1.65 difference in calculated ventilation rates does not, however, manifest itself in the calculation of the surrogate-module leak rates, because the latter depends on the ratio of the oc- to pt-concentrations. Thus, for both the integral fit and the derivative fit results, there is no statistically significant difference between the two BATS. This is a very important attribute of the tracer technique for determining leak rates.

Table 6

Leak Rates from Programmable Sampler (BATS) Results

Run No.	Time Period	Leak Rate and Standard Deviation, mL/min		
		Steady State	Integral Fit	Derivative Fit
BATS near DTA:				
	1000-1100	0.22 ± 0.06	0.20 ± 0.06	0.18 ± 0.07
1	1100-1130	0.93	1.31 ± 0.06	1.16 ± 0.09
2	1130-1200	7.43	10.29 ± 0.70	9.29 ± 1.50
3	1200-1230	2.45 ± 0.69	-0.47 ± 0.02	1.28 ± 0.68
BATS across room:				
	1015-1100	0.10 ± 0.01	0.09 ± 0.00	0.08 ± 0.02
1	1100-1130	0.83	1.22 ± 0.03	1.20 ± 0.21
2	1130-1200	6.90	9.65 ± 0.49	9.35 ± 1.39
3	1200-1230	1.73 ± 0.28	-0.42 ± 0.03	-0.84 ± 0.62

Discussion of Leak Rate Results

Six calculational determinations were made of the leak rates set by Boeing during each of the three morning runs and two (by the DTA only) of the afternoon run. The determinations were not entirely independent since the same set of data was used in two ways--the integral fit and the derivative fit.

The results were averaged, weighted by their respective uncertainties, and are shown in Table 7. Assuming that the pre-Run No. 1 leak rate of 0.09 mL/min persisted at least into run no. 1, then it should be subtracted from the first run. The best measurement of the leak rates for runs 1 and 2 are then 1.15 ± 0.09 and 9.8 ± 0.7 mL/min, i.e., very near 1 and 10 mL/min. The uncertainty of these values is about ± 5 to ± 7%, about as good as this technology can provide for precision and accuracy.

For run no. 3, it appears that Boeing entirely closed the "leak". The small calculated negative flow rate reflects the difficulty in determining such a change in leak rate in such a short period of time (30 min), which is also an unrealistic leak rate determination scenario.

Table 7.

Best Determination of the Surrogate-Module Leaks

Run No.	Time Period	Leak Rate,[a] mL/min
	1000 - 1100	0.09 ± 0.07
1	1100 - 1130	1.24 ± 0.06 (±5%)
2	1130 - 1200	9.82 ± 0.69 (±7%)
3	1200 - 1230	-0.45 ± 0.25
	1343 - 1405	1.7 ± 2.3
4	1405 - 1443	75.9 ± 6.1 (±8%)

[a] Standard deviation-weighted mean of all results.

Run no. 4 was performed after the building was accidentally overdosed more than 100-fold with the leaking tracer. In addition, the determination was only made with the less-precise DTA. Thus, the 8% uncertainty in the calculated flow rate of about 76 mL/min is not unreasonable.

Brookhaven is anxious to learn of the comparison of these tracer-determined leak rates with the actual settings as performed by Boeing.

LEAK PINPOINTING

Once a leak rate greater than the specification is detected in a particular module zone, then techniques must be implemented to pinpoint the location in order to diagnose the problem and facilitate repairs and/or modifications.

Pinpointing, which was not demonstrated during the January 25, 1991, test, can be performed in stages. Further compartmentalizing followed by DTA testing could rapidly localize the region of the leak. In addition, passive sampling could be implemented at many locations along suspected seals; several hours later or the next day analyses would point to hot spots. Such testing would be done in the absence of air mixing (fans off).

Subsequently, the Brookhaven real-time continuously operating perfluorocarbon sniffer (COPS) with a 10-second response time could then be used to pinpoint the exact location. Specially molded devices could be used with the COPS to cover larger sections of seals rather than relying solely on manual pinpointing which could be operator-biased.

CONCLUSIONS

The leak detection demonstration performed at MSFC on January 25, 1991, successfully demonstrated that leaks as small as 1 mL/min (0.06 L/h or 0.017 mL/s) could be rapidly detected with a real-time analyzer in as little as 30 min. Subsequent analysis of collected samples confirmed the real-time instrument results and showed that an overall accuracy and precision of about ±10 to ±15% is attainable with the PFT technology.

A section on the theory of leak quantification showed that, although leak rates could be quantified even when the system had not attained steady state tracer concentrations, the solutions are much more tedious and prone to greater error. The sampler steady state solution can be applied by just collecting data from about the third to fifth hours after the module testing has commenced. Self-checking of the tracer-determined leak rates was provided by applying the tracer model to the determination of the building volume, estimated to be 4450 ± 260 m^3, close to the physical size.

The leak rates in the four run periods were found to be 1.15 ± 0.09, 9.8 ± 0.7, and -0.4 ± 0.3 mL/min for the first three runs, consistent with the use of the 0 to 10 mL/min transducer and 76 ± 6 mL/min for the fourth run which used the 0 to 100 mL/min transducer.

Appendix A showed that the present limit-of-detection of the Brookhaven laboratory GC for the determination of the leaking tracer, ocPDCH, is about 0.05 fL, that is, about 0.05 x 10^{-15} liters. This is about 100-fold better than the present version of the real-time DTA; this unit can be improved to approach the laboratory GC capability.

The solution of the leak rate equations applied to a multizone Leak Certification Facility is provided in Appendix B. The leak rates and their uncertainties can be determined in a one to two hour period following attainment of steady state, which takes about 3 to 4 hours. The Leak Certification Facility is described showing that compartmentalized leaks down to a practical limit-of-detection (LOD) of 0.00002 mL/s (0.000075 L/h) is attainable.

Permeation of tracer or air through elastomer seals on the module is expected to occur at equivalent leak rates less than the above LOD (cf. Appendix C) and is, therefore, not of consequence.

A new concept of seal integrity certification has been proposed. As shown in Appendix D, examples of high structural integrity leaks have an almost linear dependence of leak rate on pressure differential. However, leak devices with poor structural integrity have power dependencies on pressure from 1.5 to 2.5. The concept is proposed to determine the seal integrity on SSF modules by determining their pressure dependence. Additionally, the magnitude of the leak rates and their dependence on pressure can also be rapidly determined while subjecting the module to other external force-generating parameters such as vibration, torque, solar gain, etc.

In conclusion, the PFT technology has already introduced a new specification capability for leak rate certification that exceeds the previous specification by 5 orders-of-magnitude. A new specification of seal-integrity certification holds the promise of even greater safety and reliability for the future Space Station Freedom.

REFERENCES

1. J. Coots, M. Klein, T. Slama, and P. Hedges. Development, qualifications and acceptance leak rate testing for the Space Station Freedom. Viewgraphs, December 11, 1990.
2. R. N. Dietz. Space Station Freedom module leak certification. Viewgraphs, December 11, 1990.
3. R. N. Dietz. Perfluorocarbon tracer technology. In *Regional and Long-Range Transport of Air Pollution*, S. Sandroni, Ed., pp. 215-247, Elsevier Science Publishers B.V., Amsterdam, The Netherlands, 1987. (Lectures of a Joint Research Centre Course, Ispra, Italy, September 15-17, 1986).
4. T. W. D'Ottavio, R. W. Goodrich, and R. N. Dietz. Perfluorocarbon measurement using an automated duel trap analyzer. *Environ. Sci. Technol.* 20 (1), 100-104 (1986).
5. R. N. Dietz, R. W. Goodrich, E. A. Cote, and R. F. Wieser. Detailed description and performance of a passive perfluorocarbon tracer system for building ventilation and air exchange measurements. In *Measured Air Leakage of Buildings*, ASTM STP 904, H. R. Trechsel and P. L. Lagus, Eds., pp. 203-264, American Society for Testing and Materials, Philadelphia, 1986.
6. E. Whittaker and G. Robinson. *The Calculus of Observations*, Blackie and Son Limited, London, 1946.
7. R. N. Dietz and E. A. Cote. Air infiltration measurements in a home using a convenient perfluorocarbon tracer technique. *Environ. Internat.* 8, 419-433 (1982).
8. R. N. Dietz. Development and testing of a Space Station Freedom module leak certification facility. A proposal, April 1991.
9. T. W. D'Ottavio, G. I. Senum, and R. N. Dietz. Error analysis techniques for perfluorocarbon tracer-derived multizone ventilation rates. Informal Report, BNL 39867, June 1987; *Bldg. Environ.* 23 (3), 187-194 (1988).
10. G. I. Senum, R. P. Gergley, E. M. Ferreri, M. W. Greene, and R. N. Dietz. Final report of the evaluation of vapor taggants and substrates for the tagging of blasting caps. Formal Report, BNL 51232, 1980.

11. M. Steinberg and R. N. Dietz. Sr^{90} ozone generator. Informal Report, BNL 14199, Nov. 1969.

12. R. N. Dietz and J. D. Smith. Calibration of permeation and diffusion devices by an absolute pressure method. In *Calibration in Air Monitoring*, ASTM STP 598, pp. 164-179, American Society for Testing and Materials, 1976.

13. R. N. Dietz, E. A. Cote, and J. D. Smith. New method for calibration of permeation wafer and diffusion devices. *Anal. Chem.* 46, 315-318 (1974).

APPENDIX A

GC DETECTION CAPABILITY FOR PFTs

When using tracers to measure leak rates, the better the limit-of-detection (LOD) of the analysis system the smaller the leak that can be measured and the more-rapidly the determination can be made. This ability to rapidly "see" the leaking tracer from a small surrogate-module leak occurring in the large building of this test using the laboratory GC system will be shown in this section. The capability being demonstrated here is an indicator of the system that can be employed for future leak certification of the SSF modules.

This appendix shows the ability to "see" the tracer concentration increasing with time in both runs 1 and 2 and also shows the ultimate limit-of-detection for the leaking tracer, using both the DTA and the laboratory GC system. The latter information will be used in the next appendix on the determination of the practical limits for surrogate-module leak detection in a real scenario.

CHROMATOGRAMS

The samples collected by the programmable Brookhaven Atmospheric Tracer Samplers (BATS) during the module leak detection demonstration were analyzed on the laboratory GC in the Tracer Technology Center at Brookhaven. The figures that follow are of the resulting chromatograms for runs 1 and 2 from the BATS located across the room from the DTA (data file 7338B), since it was shown to be the more representative sampling location. However, as shown in Tables 3 and 4 for these two runs, although the ocPDCH at the DTA site is, on average, 0.70 ± 0.10 of that at the site across the room, the oc/pt ratio for the two sites, respectively, is identical (1.03 ± 0.12); thus, the chromatograms from the BATS unit across the room can be directly compared to the DTA chromatograms shown in Figures 8 and 9.

The window of the chromatograms chosen to be shown, from 3.3 to 6.0 min, includes the peak for the leaking tracer, ocPDCH (the first named peak) and that for the reference tracer, ptPDCH (the third named peak). The middle peak, pcPDCH, is the other isomer of the reference tracer; it is not quantified because it elutes at close to the same time as the leaking tracer's other isomer, otPDCH.

Thus, the focus should be on comparing the height of the first peak to the third peak. To facilitate the comparison, all the plots have been normalized to the same reference peak height. Therefore, the leaking tracer peak heights have been automatically normalized.

Run No. 1

Figure A-1 shows two chromatograms--one from the analysis of the sample collected just before the start of the run and the other from the first of the three 10-min samples collected during the 30-min run period; Figure A-2 shows the chromatograms from the 2nd and 3rd (the last) samples of the run. The growth of the ocPDCH peak (the leaking tracer) is clearly evident.

Comparing these chromatograms to the five 6-min samples collected by the DTA during the same run (cf. Figure 8), it appears that the growth of the ocPDCH relative to the ptPDCH is identical; in actuality they are within 10% of each other. One significant difference, however, is the peak resolution, that is, the degree of separation of the individual tracer peaks. On the laboratory GC, the ocPDCH is well-separated from the other PDCH isomers; even the pPDCH isomers, the 2nd and 3rd peaks, are completely resolved, which is not the case on the DTA as it currently exists.

By a 10-fold amplification of the chromatograms of Figures A-1 and A-2, using the PE Nelson software which is part of the BNL laboratory GC system, the growth of the ocPDCH is even more clearly seen (cf. Figures A-3 and A-4). Referring to the text, it was shown that this rate of growth corresponded to a leak rate of about 1.15 mL/min (0.019 mL/s).

Run No. 2

In the same way, the three chromatograms from the BATS analyses of run no. 2 (cf. Figure A-5) can be compared to the five analyses by the DTA in the same period (cf. Figure 9). The growth of the ocPDCH is readily seen in both figures; also the heights of the oc- and ptPDCH are about equal in the last 10 minutes as seen by the third chromatogram in Figure A-5 and the average of the last two 6-min chromatogram samples in Figure 9.

Plot of data file: A:7338B7.PTS
Date: 03-15-1991 Time: 22:58:57
Sample Name: 2052BNL-NASA
Start Time= 3.30Stop Time = 6.05Min. Scale= 5678Max. Scale= 17342

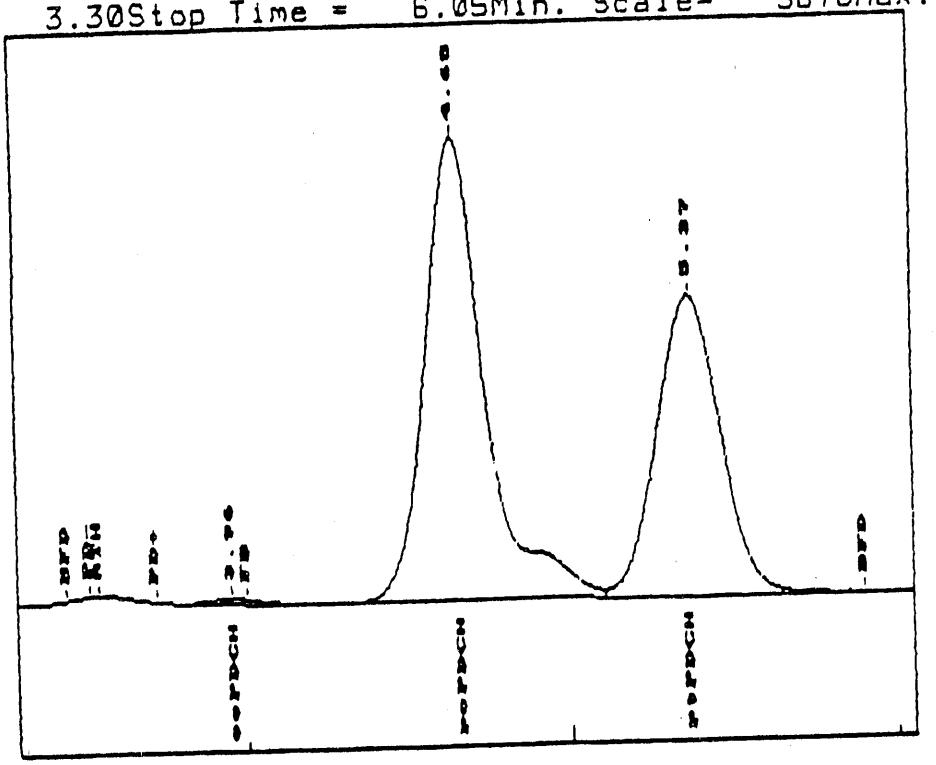

Plot of data file: A:7338B8.PTS
Date: 03-15-1991 Time: 23:00:56
Sample Name: 2052BNL-NASA
Start Time= 3.30Stop Time = 6.00Min. Scale= 5678Max. Scale= 14564

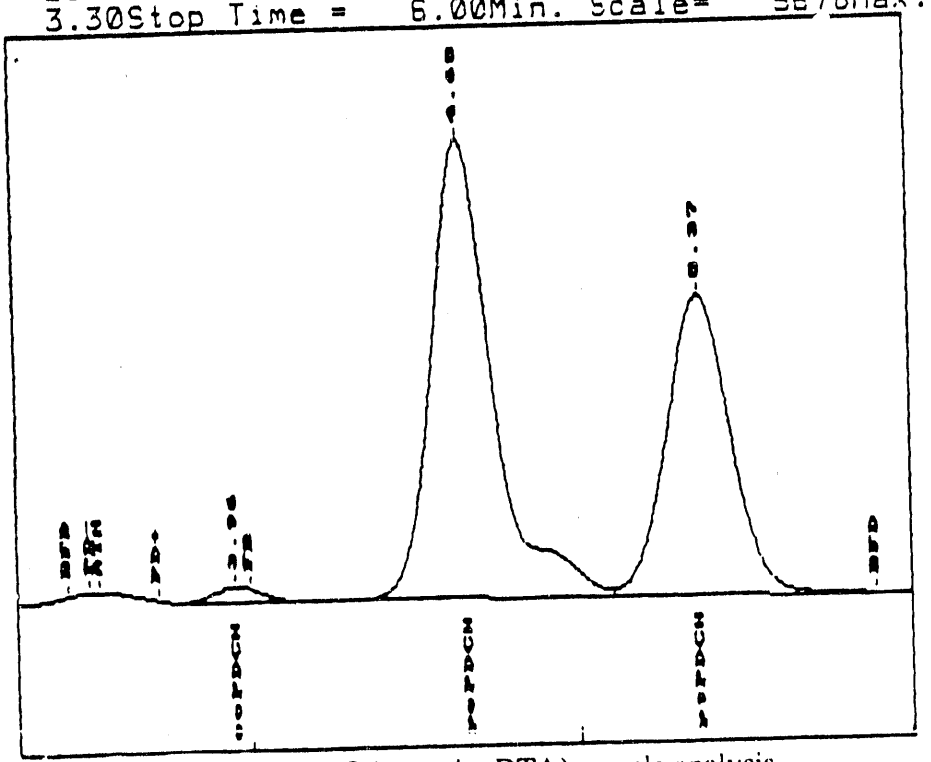

Figure A-1. BATS (opposite DTA) sa.nple analysis chromatograms just before and after the start of run no. 1.

Plot of data file: A:7338B9.PTS
Date: 03-15-1991 Time: 23:03:28
Sample Name: 2052BNL-NASA
Start Time= 3.30Stop Time = 6.00Min. Scale= 5645Max. Scale= 13903

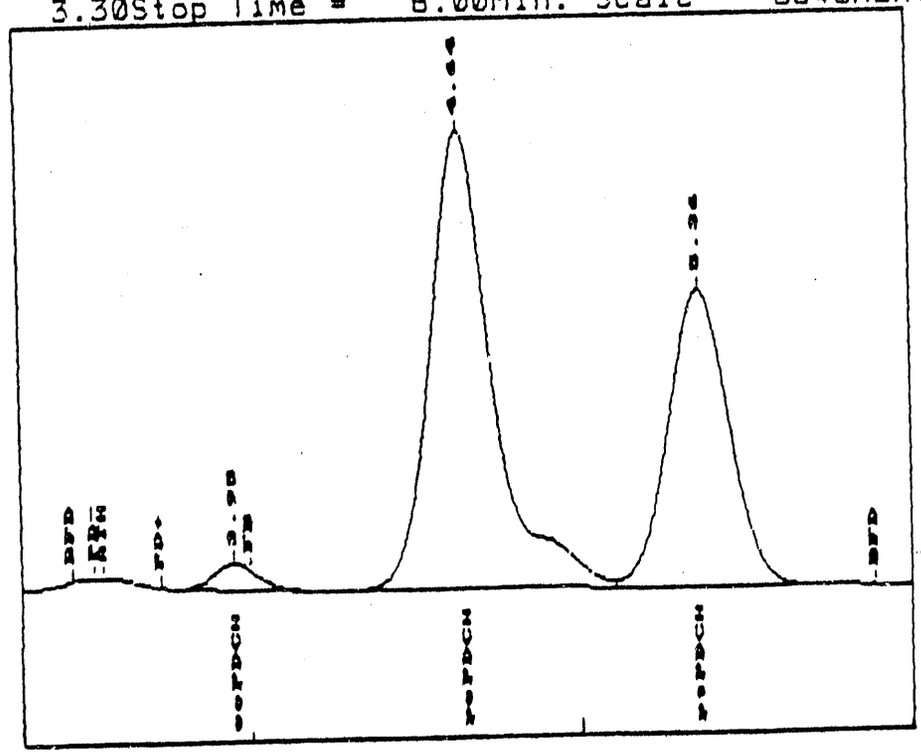

Plot of data file: A:7338B10.PTS
Date: 03-15-1991 Time: 23:05:25
Sample Name: 2052BNL-NASA
Start Time= 3.30Stop Time = 6.00Min. Scale= 5658Max. Scale= 15396

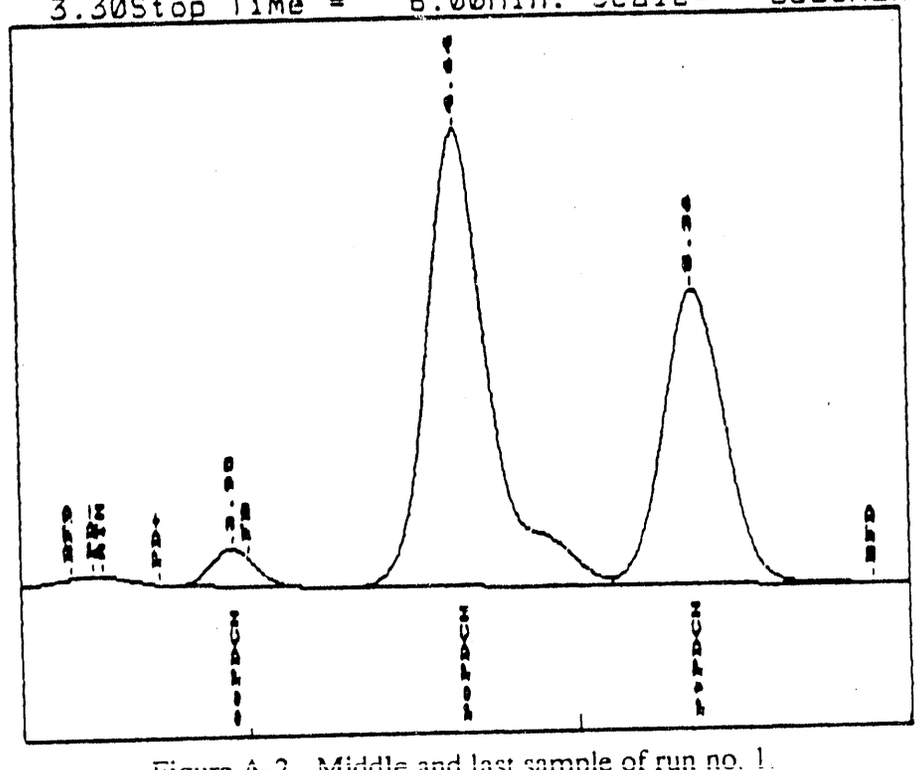

Figure A-2. Middle and last sample of run no. 1.

Plot of data file: A:7338B7.PTS
Date: 03-15-1991 Time: 23:08:28
Sample Name: 2052BNL-NASA
Start Time= 3.30Stop Time = 6.00Min. Scale= 5680Max. Scale= 6846

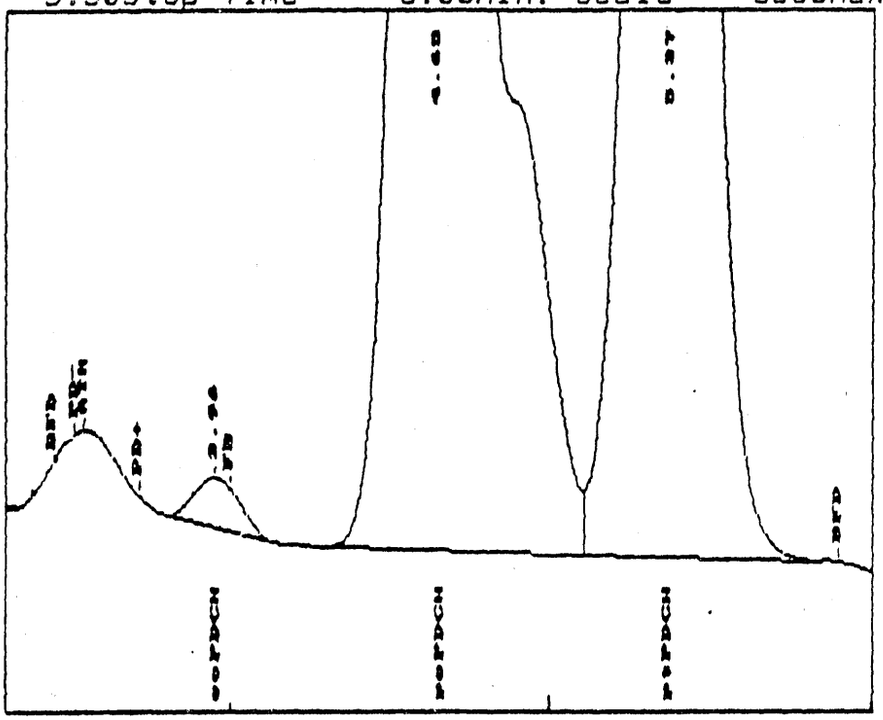

Plot of data file: A:7338B8.PTS
Date: 03-15-1991 Time: 23:10:14
Sample Name: 2052BNL-NASA
Start Time= 3.30Stop Time = 6.00Min. Scale= 5678Max. Scale= 6567

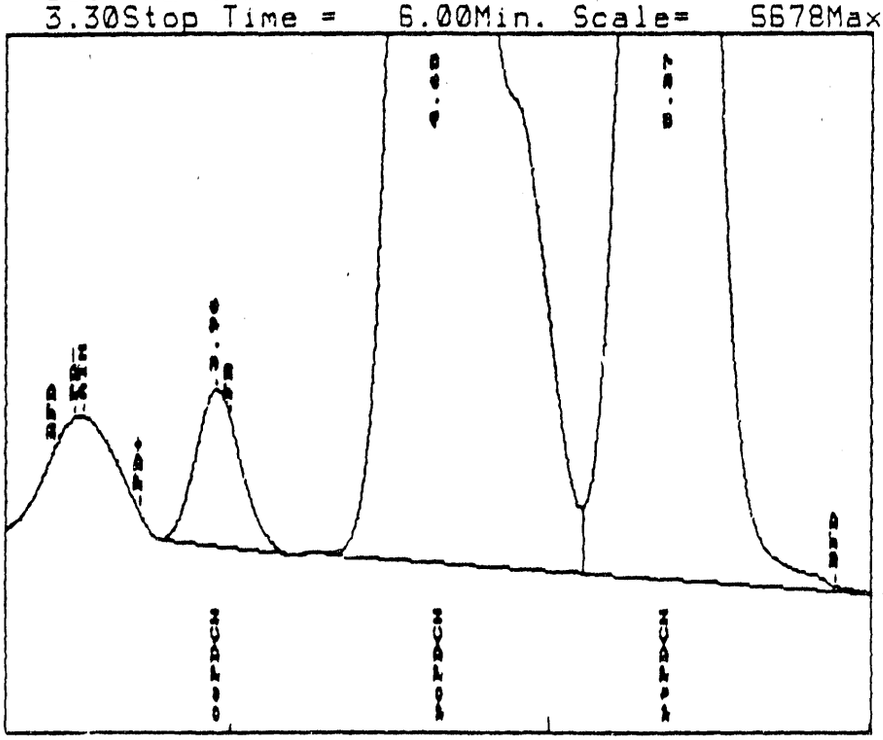

Figure A-3. Figure A-1 amplified 10-fold.

Plot of data file: A:7338B9.PTS
Date: 03-15-1991 Time: 23:12:01
Sample Name: 20S2BNL-NASA
Start Time= 3.30Stop Time = 6.00Min. Scale= 5645Max. Scale= 6471

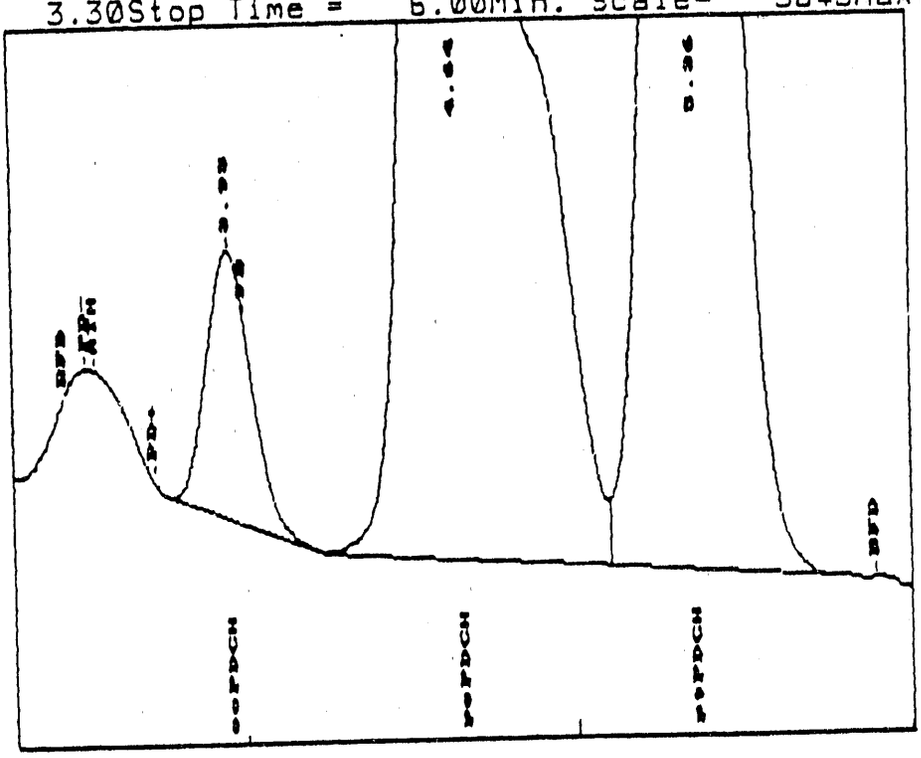

Plot of data file: A:7338B10.PTS
Date: 03-15-1991 Time: 23:14:33
Sample Name: 20S2BNL-NASA
Start Time= 3.30Stop Time = 6.02Min. Scale= 5656Max. Scale= 6630

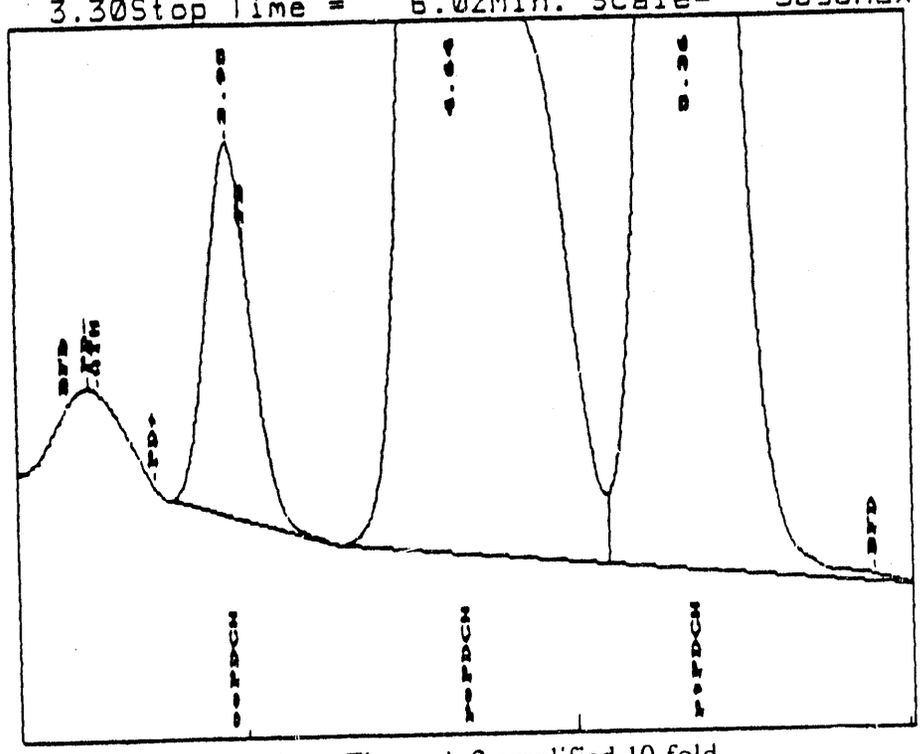

Figure A-4. Figure A-2 amplified 10-fold.

Figure A-5. Three BATS sample results from run no. 2.

Plot of data file: A:7338B11.PTS
Date: 03-15-1991 Time: 23:22:58
Sample Name: 2052BNL-NASA
Start Time= 3.30Stop Time = 6.02Min. Scale= 5659Max. Scale= 12005

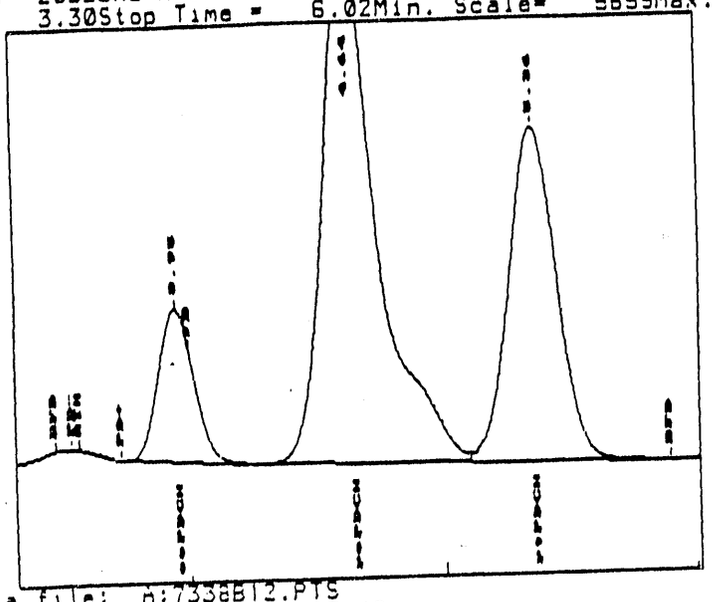

Plot of data file: A:7338B12.PTS
Date: 03-15-1991 Time: 23:23:46
Sample Name: 2052BNL-NASA
Start Time= 3.30Stop Time = 6.00Min. Scale= 5652Max. Scale= 11295

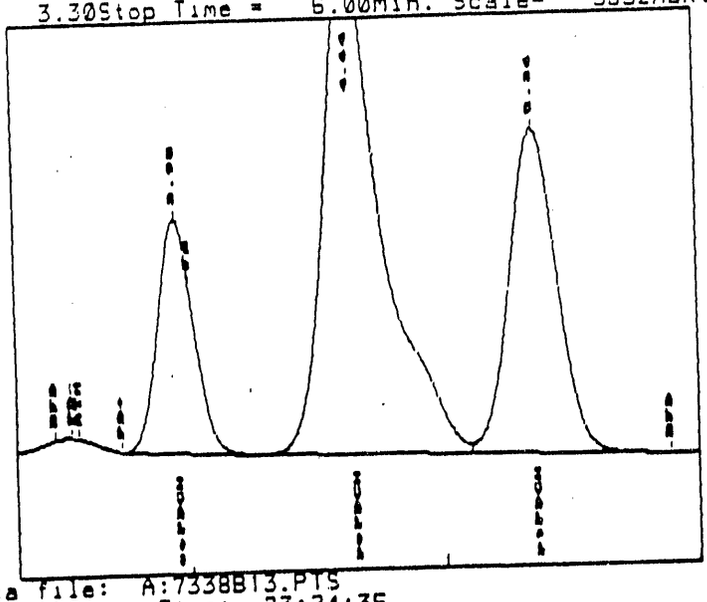

Plot of data file: A:7338B13.PTS
Date: 03-15-1991 Time: 23:24:35
Sample Name: 2052BNL-NASA
Start Time= 3.30Stop Time = 6.00Min. Scale= 5693Max. Scale= 12030

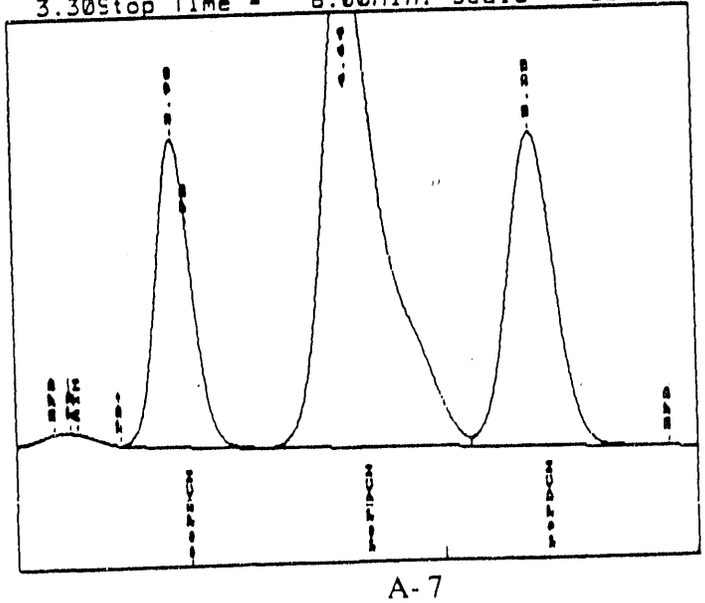

ULTIMATE PFT LIMIT-OF-DETECTION (LOD)

It is obvious from these two runs that the PFT technique can see leak rates of less than 1/100 of the original NASA leak rate specification of 2 mL/s, but--how much less is the ultimate capability? To answer that question, the ultimate LOD, or minimum discernible quantity, of the leaking tracer must first be determined.

This minimum detection capability is different for the two analysis systems used in this test--the DTA and the laboratory GC system. This section provides an estimate of that capability for both instruments. That for the current DTA is of academic interest only, since the capability of the laboratory GC could be provided in an updated DTA.

DTA Minimum Detectable Quantity

Using a definition of the limit-of-detection (LOD) as that quantity whose signal is three time the noise level in the region of the signal, it is apparent form Figure 8 that the ocPDCH peaks in the first two chromatograms are at the LOD. The two noise spikes that appear just before and at the peak elution time are of a magnitude of about 0.1 inch and the estimated height of the two peaks was 0.04- and 0.14-inches, respectively, corresponding to about 3 and 10 fL (10^{-15} liters), respectively. Thus, the LOD of the DTA as configured in this text was about 5 fL, limited, in part, by the noise spikes which were due to the switching of the backflush valve.

Laboratory GC System Minimum Detectable Quantity

The smallest ocPDCH concentration sampled by either of the two BATS used in the NASA leak detection demonstration occurred on the first sample tube of the unit near the DTA (file 7337B1 in Table 3) because it was the only sample collected from 0900 to 0915, which was well before any work commenced with the leaking tracer.

As indicated in the text, this sample was at ambient levels for the PMCH and ocPDCH but 3 to 4 times ambient for the ptPDCH and PMCP, the two reference tracers, because some of their vapors got into the building ahead of the official installation time of 0930.

In this section, the chromatogram of this sample in the PDCH isomer window (3.3 to 6.0 min) will be examined and then the ocPDCH will be used to estimate the laboratory GC system LOD.

Chromatogram of File 7337B1. A peak not resolved in the earlier shown chromatograms of Figures A-1 to A-5 is shown in the chromatogram of this sample (cf. upper chromatograms of Figure A-6) at a retention time of 4.90 min (labelled mcPDCH). This component is present in the ambient air at about 6.8 ± 0.3 fL/L; in the later chromatograms it was masked by the much higher concentrations of the nearby pcPDCH peak from the reference tracer. The concentration represented by this peak (after correcting for a small amount present in the reference tracer) corresponds to 8.8 fL/L, close to the expected ambient level of 6.8 fL/L.

The ocPDCH concentration of 0.24 fL/L in Table 3 for this sample had been corrected for a contribution from the reference tracer; the peak actually corresponds to a concentration of about 0.26 fL/L. Since the sample volume was 0.8 L, the quantity of ocPDCH represented by the peak is 0.21 fL (0.21×10^{-15} liters). The upper chromatogram of Figure A-6 was amplified 25-fold using the PE Nelson software to produce the lower chromatogram. Clearly, 0.21 fL of the leaking tracer is readily determinable.

Limit-of-Detection (LOD). By electronically expanding the picture around the ocPDCH peak, the chromatogram of Figure A-7 was produced (about a 50% increase in amplitude but a 3-fold expansion of the time axis). The baseline shown under the ocPDCH was that drawn automatically by the PE Nelson software giving a peak area of 88.8 μV-seconds, as shown in the table under the chromatogram.

Each horizontal line in the chromatogram represents 1 μV, which is the resolution of the PE Nelson data acquisition system. The noise at the baseline just before and at the top of the ocPDCH peak is about ± 1 μV. This is an enhanced capability of the Brookhaven version brought about by the use of an analogue electronic energy-input variable frequency filter ahead of the digital data acquisition system. The noise-smoothed peak height for the 0.21 fL quantity is 12 μV or 12 times noise. Thus, noise corresponds to ± 0.02 fL and the LOD, defined as 3 x Noise (3 μV high), is about 0.05 fL ocPDCH. This is 100-fold more resolving power than the present DTA.

Plot of data file: A:7337B1.PTS
Date: 03-15-1991 Time: 23:39:50
Sample Name: 2005BNL-NASA
Start Time= 3.30Stop Time = 6.00Min. Scale= 5564Max. Scale= 6282

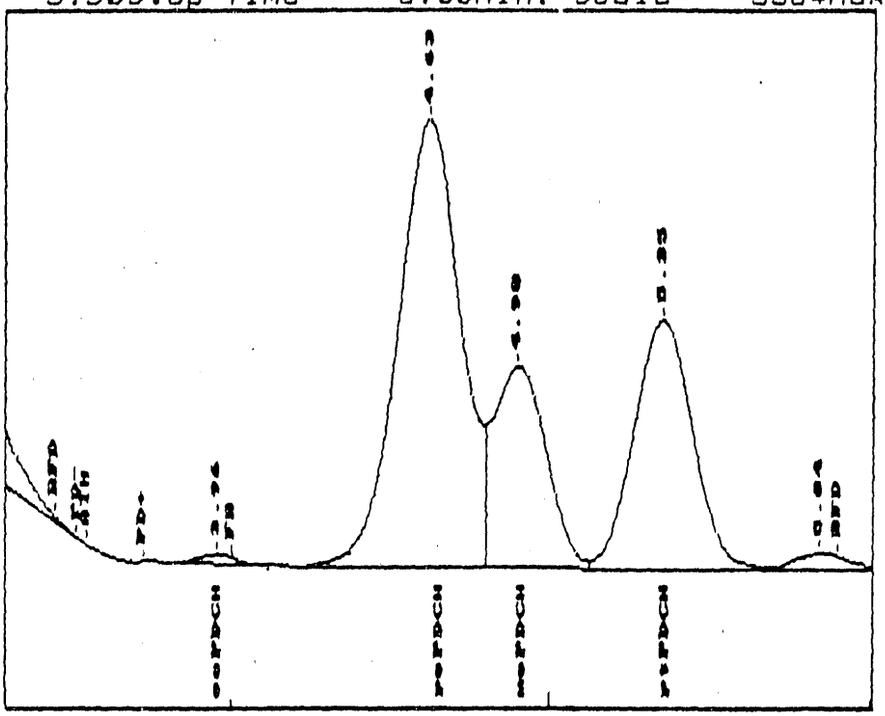

Plot of data file: A:7337B1.PTS
Date: 03-15-1991 Time: 23:42:52
Sample Name: 2005BNL-NASA
Start Time= 3.30Stop Time = 6.02Min. Scale= 5564Max. Scale= 5593

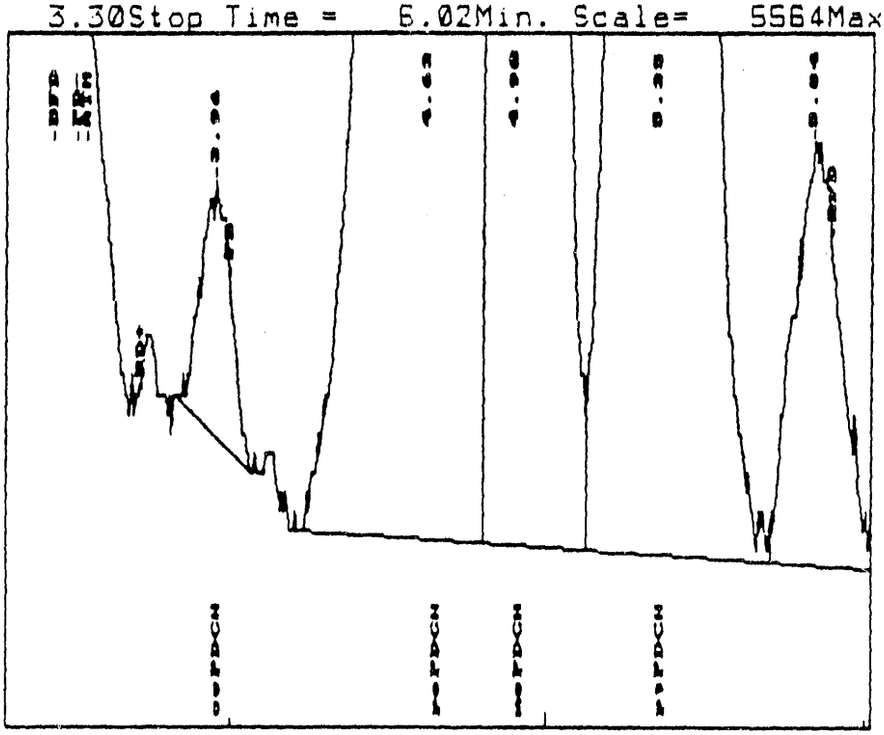

Figure A-6. Analysis of building background tracer levels.

Plot of data file: A:7337B1.PTS
Date: 03-15-1991 Time: 23:48:32
Sample Name: 200SBNL-NASA
Start Time= 3.48Stop Time = 4.40Min. Scale= 5570Max. Scale= 5589

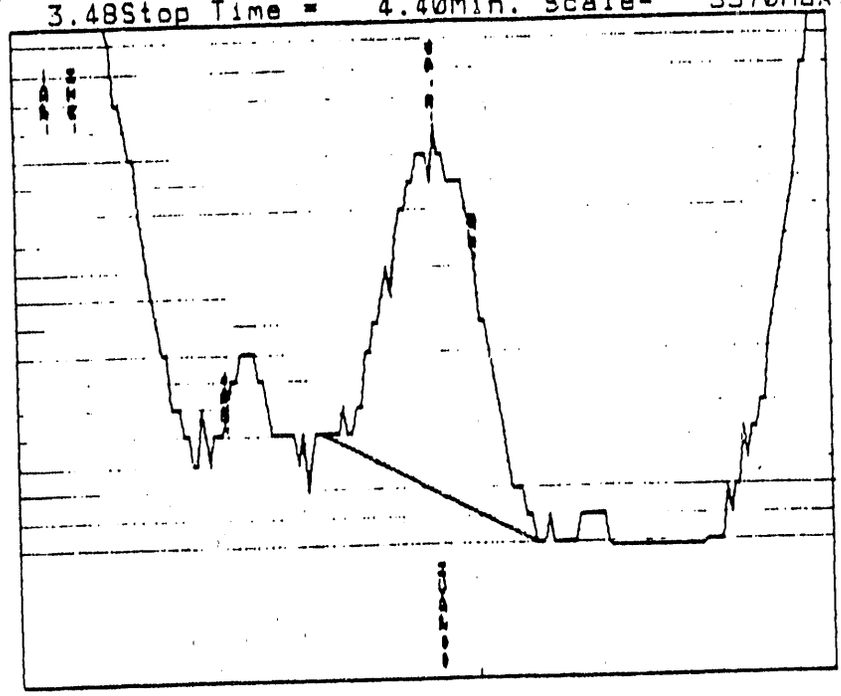

EXTERNAL STANDARD TABLE

03-15-1991 23:49:23 Version 4.1

Data File: A:7337B1

Sample Name: 200SBNL-NASA
Date: 01-28-1991 09:04:22 Method: 6A160F8 03-15-1991 23:36:54 # 55
Interface: 0 Cycle#: 1 Operator RWG Channel#: 0 Vial#: N.A.
Starting Peak Width: 3 Threshold: .2 Area Threshold: 5

Instrument Type: Varian 6000-2481 (1) Column Type: SP1000
Solvent Description:
Conditions: 160 C Isotermal
Detector 0: ECD Ni 63 Detector 1: None
Misc. Information: LPT1:

Starting Delay: 1.00 Ending retention time: 13.60
Area reject: 50 One sample per 0.300 sec
Amount injected: 1.00 Dilution factor: 1.00
Sample Weight: 1.000000

PEAK NUM	RET TIME	PEAK NAME	CONCENTRATION in ****	NORMALIZED CONC	AREA	HEIGHT	AREA/ HEIGHT	BL	REF PEAK	% DELTA RET TIME	CONC/AREA
1	1.150		97.8000	0.1279%	90	22	4.4	1			1.0000E+00
3	1.570	PMCP	2356.0830	3.0810%	2356	422	5.6	2	0	1.290	1.0000E+00
4	1.890		49663.6910	64.9431%	49664	1484	33.5	2			1.0000E+00
5	2.890		6929.1001	9.0609%	6929	208	33.2	1			1.0000E+00
6	3.955	ocPDCH	88.8000	0.1161%	89	13	6.7	1	0	-.1262	1.0000E+00
7	4.625	pcPDCH	7878.9648	10.3030%	7879	573	13.7	2	0	-.7510	1.0000E+00
8	4.900	mcPDCH	2965.1907	3.8775%	2965	257	11.5	2	0	-.4065	1.0000E+00
9	5.350	ptPDCH	3973.6689	5.1962%	3974	317	12.5	2	0	-.1865	1.0000E+00
10	5.840		221.5688	0.2897%	222	22	10.2	2			1.0000E+00
11	7.320		315.1500	0.4121%	315	13	23.8	1			1.0000E+00
12	7.905		197.1000	0.2577%	197	13	14.8	1			1.0000E+00
13	8.790		1785.1501	2.3348%	1785	43	12.0	1			1.0000E+00

TOTAL AMOUNT = 76472.5700

Figure A-7. Chromatogram of ocPDCH showing its limit-of -detection.

APPENDIX B

PRACTICAL LIMITS FOR MULTI-LOCATION MODULE LEAK CERTIFICATION

The testing that was performed in the January 25, 1991, surrogate-module leak detection demonstration was performed on a very small "module" located in a very large, leaky building. Both ends of the building contained "dead" zones in which the air was not well-mixed with the rest of the open area. Even the mixing in the open area was not perfect; certain locations were biased by the local influx of outside air.

The purpose of this appendix is to provide some practical guidelines to the manner in which module leak certification should be performed and to demonstrate how to maximize the ability to "see" the smallest possible leak in a module in a reasonable period of time, i.e., a few hours.

As shown in the text, the demonstration was performed under time-dependent conditions of changing concentrations of the leaking tracer. The objective of this appendix is to present brief descriptions of 1) the advantages of the simplifying steady-state approach, 2) the steady-state multizone solution and error analysis, 3) the proposed leak certification facility, 4) the dependence on testing duration, and 5) the optimization of the tracer concentration within the module. The magnitude of leaks that can be detected as a function of these parameters will be presented in tabular form.

The goal of this appendix is to demonstrate that practical certification of the leak-tightness of modules to very low rates can be attained in a few hours and that, if the leak specification is not attained, the ability to find the joint or seal that has failed can be expedited with the multizone capability of the PFT technology.

ADVANTAGES OF ATTAINING STEADY STATE

As shown in the theory section on leak quantification, the exact solution of the material balance equation for a leak or leaks occurring into a single zone or volume of a building can be performed by the derivative or integral fit to Eq. (4), but the steady state solution is much simpler

$$R_\ell = \frac{C_\ell S_r}{C_r C_{mi}} \tag{7}$$

The time to attain steady state is a function of τ, the turnover time, which was 0.4 h in the recent demonstration in the 4500-m^3 building. Thus, 95 to 98% of steady state was attained in just 3τ or 4τ, i.e., 1.2 to 1.6 h. However, whether the time-dependent or steady-state solution is being used, the models all assume that the leaking tracer is well-mixed, that is, instantaneously at the same concentration in all locations. Since the building was equipped with one floor fan of about 5000 cfm (150 m^3/min) capacity, the time required to mix the air just once in the building was 30 min. At least three or four complete mixes of the building air would be required to be well-mixed, i.e., 1.5 to 2 hours. Hence, one might as well wait that time and use the simpler steady-state solution.

Lastly, although it could be assumed, the exact solution of the time-dependent equations for the case of multiple zones is quite extensive and beyond the scope of this report. That for the case of the steady-state solution in multiple zones will be given next.

STEADY-STATE MULTIZONE SOLUTION

The proposed facility (described in the next section) for quantifying module leak rates will comprise three zones--one housing each end of the module and a third housing the middle section. Similar to the January 25, 1991, test, the air in the zone housing the module will be tagged with a tracer, but since there are three proposed zones, three different reference tracers will be used, so that all the air flow rates into the zone from adjacent zones and from outside and all air flow rates out of each zone into adjacent zones and into the outside air can be computed.

Again, as in the case of the single zone test, a material balance for the leaking tracer results in N equations containing three terms--the concentrations of the leaking tracer in each zone (measured), the interzonal flow rates (calculated above from the zonal tracers), and the unknown source rates of the leaking tracer into each zone, which can now be calculated and from which, by dividing by the leaking tracer's concentration within the module, the rates of the leaks into each zone can be determined.

The purposes of this section is to provide the solution, in matrix notation, to the ventilation flow rate determinations in the leak facility zones and to their corresponding uncertainties and then to show how the flow equations are used to solve the matrix equation for the leaking tracer rates in each zone and their uncertainties.

The Ventilation Solution and Error Analysis

The ventilation flows are computed by inserting the measured reference tracer concentrations and the known reference tracer emissions rates into the mass balance and flow balance equations for each zone of the leak facility. In general, for N well-mixed zones, there are N^2 mass balance and 2N+1 air flow balance equations to solve in calculating the ventilation quantities of interest. It can be shown[9] that the tracer mass balance equations and the air flow balance equations can be combined into the following single matrix equation for the general N-zone case:

$$\begin{bmatrix} -1 & 1 & 1 & \bullet & \bullet & 1 \\ 0 & C_{11} & C_{12} & \bullet & \bullet & C_{1N} \\ 0 & C_{21} & C_{22} & \bullet & \bullet & C_{2N} \\ \bullet & \bullet & \bullet & \bullet & \bullet & \bullet \\ \bullet & \bullet & \bullet & \bullet & \bullet & \bullet \\ 0 & C_{N1} & C_{N2} & \bullet & \bullet & C_{NN} \end{bmatrix} \begin{bmatrix} R_{00} & R_{01} & R_{02} & \bullet & \bullet & R_{0N} \\ R_{10} & R_{11} & -R_{12} & \bullet & \bullet & -R_{1N} \\ R_{20} & -R_{21} & R22 & \bullet & \bullet & -R_{2N} \\ \bullet & \bullet & \bullet & \bullet & \bullet & \bullet \\ \bullet & \bullet & \bullet & \bullet & \bullet & \bullet \\ R_{N0} & -R_{N1} & -R_{N2} & \bullet & \bullet & R_{NN} \end{bmatrix} = \begin{bmatrix} 0 & 0 & 0 & \bullet & \bullet & 0 \\ S_{r1} & S_{r1} & 0 & \bullet & \bullet & 0 \\ S_{r2} & 0 & S_{r2} & \bullet & \bullet & 0 \\ \bullet & \bullet & \bullet & \bullet & \bullet & \bullet \\ \bullet & \bullet & \bullet & \bullet & \bullet & \bullet \\ S_{rN} & 0 & 0 & \bullet & \bullet & S_{rN} \end{bmatrix} \quad \text{(B-1)}$$

where R_{ij} = rate of air flow from zone i to zone j ($i \neq j$, zone 0 = outdoors)

R_{ii} = sum of all air flows into zone i ($i > 0$)

R_{00} = sum of all infiltration flows = ΣR_{0i}

C_{ij} = concentration of reference tracer i in zone j ($C_{i0} = 0$)

S_{rj} = source emission rate of the reference tracer in zone j (constant)

Using boldface to denote the matrices, this equation becomes

$$\mathbf{C_r R = S_r} \quad \text{(B-2)}$$

which can be solved for the air flow rate by using the identity equation

$$\mathbf{C_r^{-1} C_r = I}$$

Left multiplying Eq. (B-2) by the inverse of the reference tracer concentration matrix, $\mathbf{C_r^{-1}}$, gives

$$\mathbf{C_r^{-1} C_r R = R = C_r^{-1} S_r} \quad \text{(B-3)}$$

The errors or uncertainties associated with the individual rates in the **R** matrix were estimated from a first order error analysis.[9] Taking the derivative of Eq. (B-3), it can be shown that

$$\Delta R = \left[\left(C_r^{-1} \right)^2 \Delta S_r^2 + \left(C_r^{-1} \right)^2 \Delta C_r^2 R^2 \right]^{1/2} \qquad \text{(B-4)}$$

where ΔR = matrix ventilation flow errors (standard deviations),

ΔS_r = matrix of estimated source emission rate errors of the reference tracers,

ΔC_r = matrix of estimated reference tracer concentration errors, and

C_r^{-1} = inverse of the reference tracer concentration matrix.

The notation of a matrix squared (e.g., ΔS_r^2 and $\left(C_r^{-1} \right)^2$) means to square each element of the matrix, not to multiply the matrix by itself. Similarly, the square-root notation means to take the square root of each element of the matrix. In addition, the ΔC_r matrix is formed in the same manner as the C_r matrix except that all the elements of the first row and first column are set to 0.

The Leaking Tracer Solution and Error Analysis

An equation similar to Eq. (B-2) can be written for the leaking tracer:

$$C_\ell R = S_\ell \qquad \text{(B-5)}$$

where the matrix dimensions for **R** in this case is N by N, that is, the first row and first column in Eq. (B-1) has been dropped. Since there is only one leaking tracer concentration and one total leaking tracer rate in each zone, defined by C_ℓ and S_ℓ, respectively, they are one row-by N column-matrices, respectively.

The direct solution for S_ℓ, the desired leaking tracer rates in each zone, can be obtained by substituting Eq. (B-3) into Eq. (B-5) giving

$$S_\ell = C_\ell C_r^{-1} S_r \qquad \text{(B-6)}$$

where, as for **R** above, C_r^{-1} and S_r are the N by N inverse matrix and matrix, respectively, in Eq. (B-1) formed by dropping the first row and first column of each. The module leak rates in each zone are then

$$R_\ell = \frac{1}{C_{mi}} S_\ell$$

where C_{mi} is the concentration of the leaking tracer inside the module, a constant known value. Note that the solution only makes use of the concentrations of the leaking and reference tracers and the source rates for the reference tracers.

Again the errors or uncertainties associated with the individual leaking tracer rates can be gotten by differentiating Eq. (B-6) to give

$$dS_\ell = dC_\ell C_r^{-1} S_r + C_\ell dC_r^{-1} S_r + C_\ell C_r^{-1} dS_r \qquad \text{(B-7)}$$

Since the errors of the inverse of the reference tracer concentration matrix, i.e., dC_r^{-1}, cannot be estimated, it is eliminated by using the differential of the identity matrix giving

$$dC_r^{-1} C_r + C_r^{-1} dC_r = 0$$

Solving by transposing and right-multiplying by C_r^{-1} gives

$$dC_r^{-1} = -C_r^{-1} dC_r C_r^{-1}$$

Substituting into Eq. (B-7) and squaring the individual matrix element terms yields the error expression

$$\Delta S_\ell = \left[\Delta C_\ell^2 \left(C_\ell^{-1}\right)^2 S_r^2 + C_\ell^2 \left(C_\ell^{-1}\right)^2 \Delta C_\ell^2 \left(C_\ell^{-1}\right)^2 S_\ell^2 + C_\ell^2 \left(C_\ell^{-1}\right)^2 \Delta S_\ell^2 \right]^{1/2} \qquad \text{(B-8)}$$

Thus, the overall error in the leaking tracer rates is comprised of three terms:

1st term = error contribution from the leaking tracer concentration uncertainties,

2nd term = error contribution from the zonal interdependencies of the leak facility combined with the reference tracer concentration uncertainties, and

3rd term = error contribution from the reference tracer source rate uncertainties.

A complete software package can be developed to compute the module leak rates in up to three or four locations simultaneously along with the uncertainties on those rates.

PROPOSED LEAK CERTIFICATION FACILITY

Equation (7) can be used to optimize the detection of the smallest possible leaks. Substituting $R_E = S_r/C_r$ gives

$$R_\ell = \frac{C_\ell R_E}{C_{mi}} \qquad \text{(B-9)}$$

The smallest leak measurement detectable is governed by the smallest leaking tracer concentration detectable, by minimizing the zonal exfiltration rate (R_E), and maximizing the concentration within the

module (C_{mi}). This section, which addresses the configuration and volume of the zones surrounding the module, is applicable to minimizing R_E.

The exfiltration rate, which, in the case of a single zone, is a single flow rate or, in the case of multiple zones, is the sum of all flow rates out of the zone, is minimized by making the zone around the module smaller which inherently makes it tighter.

Figure B-1 provides a proposed view of the facility needed to minimize the air flow movement in the zones surrounding the module. A typical 15-foot diameter by 40-foot long module is placed in the middle of Building 4572, supported about 5-feet above the floor. Tarpaulins (shown by the dashed lines in Figure B-1) are brought to within 5- to 7-feet of the top, sides, and ends of the module to completely enclose it. Two extra canvas sheets with appropriately-sized holes to accommodate the diameter of the module are draped in a way to divide the overall tarpaulin room into three zones--zones 1 and 3 containing the ends of the module with their concomitant seals and zone 2, the middle section of the module. With this arrangement, the volume of the three zones will be about 300 m^3 (±10%) and, assuming a practical ACH of 1 h^{-1} for this arrangement, the minimum R_E will be ~300 m^3/h per zone.

Air mixing within each of the zones will be facilitated by fans below and above the module operating in a fashion to achieve a circular flow field around the module section as shown in End View A-A (Figure B-1). This should assure the requirement of the ventilation model, that is, good mixing.

The balance of the building outside the tarpaulin zones will be considered zone 4. While it will still behave as a leaky zone (during the January test its ACH was 2.5 h^{-1}), it is quite certain that the tarpaulin zones will have an ACH of 1 h^{-1} or less, thus minimizing R_E. The air in zone 4 will also be stirred in a cyclic fashion with fans placed to move air as shown in the Plan View of zone 4. Each of these four zones will be tagged with a different reference tracer, leaving one of the five available PFTs for use as the leaking tracer.

There are several self-checking advantages to this arrangement when using the models to compute both the ventilation flow rates and the module leak rates. First, because there is physically no connection between zones 1, 2, and 3 and the outside air (barring penetrations in the floor), their respective infiltration and exfiltration rates should be zero. Similarly, zone 1 is not in physical contact with zone 3, so their interzonal rates should be zero. Any deviation from this outside the bounds of the

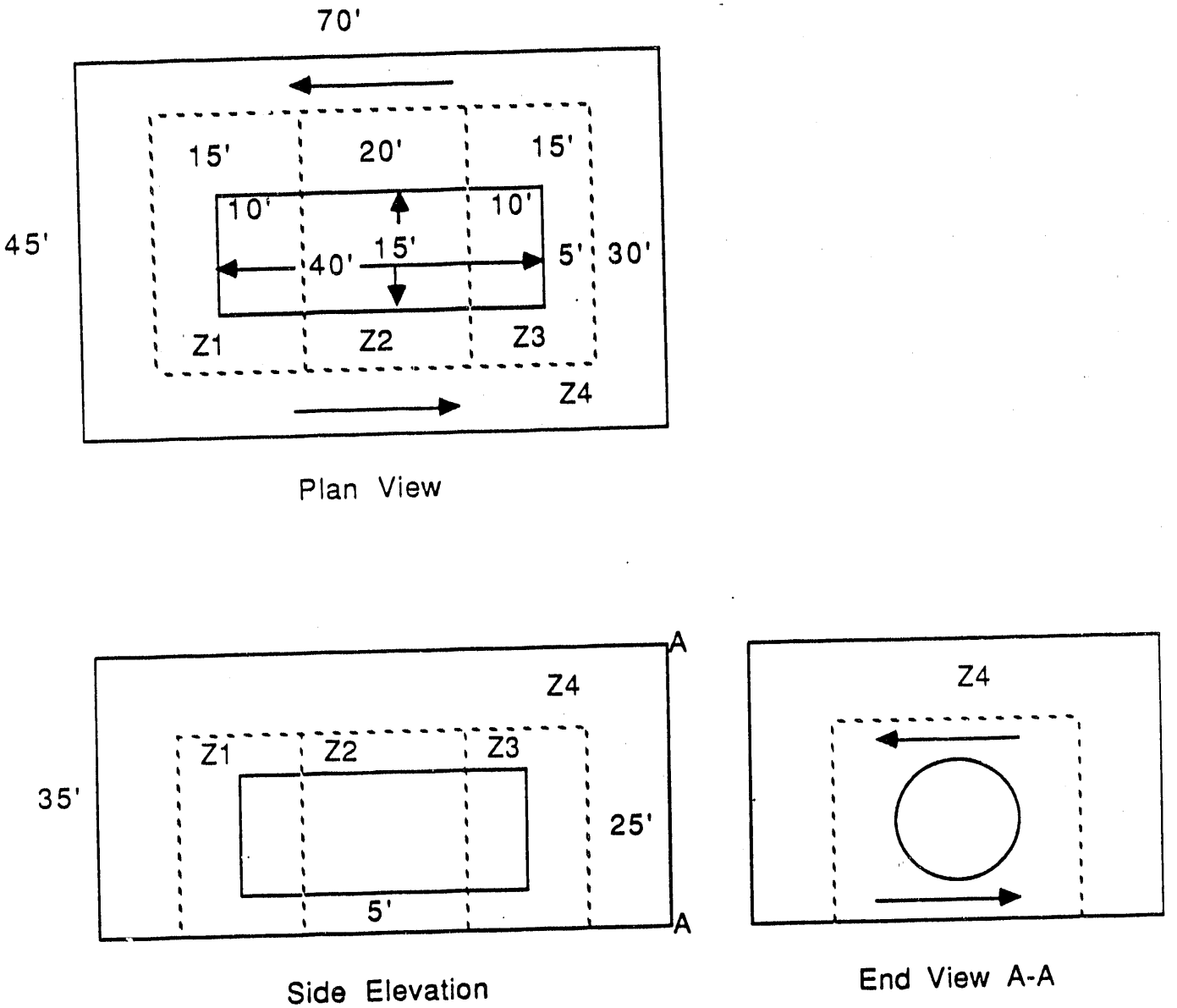

Figure B-1. View of a module in the proposed leak certification facility within Building 4572.

respectively computed flow rate uncertainties will point to a need to check the physical structure of the Leak Certification Facility.

Again, looking at Figure B-1, there is no physical connection between the module and zone 4. The only way that the leaking module tracer can be present in zone 4 is by air exchange with the other three zones, which should be accommodated by the zonal reference tracers. Thus, the solution of the module leak rate into zone 4 should accommodate zero within its uncertainty. Even if it does, the magnitude of that calculated leak rate will perhaps be an indicator of the minimum reliable leak rate capability, after correcting for the high air throughput in that zone. If it does not accommodate zero, then the physical reasons must be ascertained.

This self-checking feature should enhance the overall reliability in the output results. It can also be shown that the ultimate reliability will be obtained for a physical zonal configuration in which the interzonal flow rates are minimized. Each zone then acts as if it were a single zone. Thus, a large leak in one zone would less likely mask a small leak in another zone. This is a property of obtaining an optimal condition number near 1 for the concentration matrix.[9]

LEAK RATE DETECTABILITY OPTIMIZATION

As shown above, the other two items which influence the minimum detectable leak rate capability are the optimization of the procedures necessary to measure the smallest leaking tracer concentration and the optimization of the concentration of the leaking tracer in the module. This section will address both these considerations.

Optimizing the Detectability of the Zonal Leaking Tracer Concentration

Since a tracer concentration is determined by collecting and measuring the PFT quantity in the known volume of air sampled, the minimum determinable concentration is governed by the minimum quantity of tracer that can be seen above the ambient background level in the maximum sample volume that can be collected in a reasonable period of time given the present capability of the PFT technology.

The relevant parameters in this optimization are listed here with their appropriate values or range of values.

Parameter	Value	Comment
Leaking tracer type	ocPDCH	Highest GC detectability and low ambient concentration
C_ℓ background	0.25 fL/L	±0.05 fL/L
v_ℓ LOD	0.05 fL	See Appendix A
Max. sampling rate	200 mL/min	Near 100% efficiency
Sampling duration	6 to 60 min	<15L for 100% collection
Zonal volume	250 to 350 m^3	Minimum volume to house module
Zonal ACH	0.5 to 1.5 h^{-1}	Practical capability
Module tracer conc.	0.1 to 1 ppm oPDCH	Convenience in module tagging
- ocPDCH content	0.04 to 0.4 ppm	Based on 40% as ocPDCH

Minimum ocPDCH Discernible above Background. Since the limit-of-detection (LOD) for this PFT is 0.05 fL (see Appendix A), the minimum uncertainty in any measurement will be twice the LOD. Thus,

$$\text{min. } \sigma_v = \pm 0.10 \text{ fL}$$

and any quantity of tracer, v, determined will have the above σ_v associated with it.

When air is sampled within the module leak certification facility during a test, ocPDCH will be present both from the module leaks and the ambient background such that

$$v_T = v_\ell + v_{oa}$$

where the subscripts refer, respectively, to the total measured quantity, that from the leaking tracer, and that from the outside air. It can be shown that for an uncertainty of 0.10 fL in both v_T and v_{oa}, then the uncertainty in v_ℓ will be ± 0.14 fL. If this is to be no more than 12% of v_ℓ, then

$$v_\ell = 1.20 \text{ fL ocPDCH}$$

the minimum discernible quantity above background for a less than ±12% uncertainty.

Maximum Sample Volume in a Reasonable Period of Time. The maximum sampling rate for 100% collection efficiency with the current technology PFT sampling equipment is about 200 mL/min. Since a sample collection period on an adsorbent tube should be at least 6 min in duration to eliminate biases in the representativeness of the sample, but no more than 60 min in duration such that several

measurement periods can be performed in a reasonable period of time, the sample volume size will be from 1.2 to 12 L of air.

Optimization of the Leaking Tracer Concentration in the Module

Before Eq. (B-9) can be evaluated for the minimum detectable leak rate determination, the criteria governing the concentration of the leaking tracer must be evaluated. Obviously, the larger C_{mi} can be, the better will be the leak rate detection capability. For a 15-foot diameter by 40-foot long module (volume is 7070 ft^3 or 200 m^3), at a test pressure of 1.1 atm absolute, the module would contain the following amounts of the leaking tracer at different concentrations:

Conc. PDCH	oPDCH Quantity		
in module, ppm	Vol., L (gas)	Mass, g	Vol., mL (liquid)
100	22	360	194
10	2.2	36	19.4
1	0.22	3.6	1.94
0.1	0.022	0.36	0.194

Certainly PFT cost is not a problem. At less than $0.20 per gram in metric ton quantities and perhaps 5 times that cost in kg quantities, the cost is less than $75 to $400 even at a module concentration of 100 ppm.

In use, the gas that would be leaking out is air. Even at 100 ppm oPDCH, the composition of the air has not effectively been changed.

The real concern in working at high ppm levels is that pure liquid PFT would most likely have to be used to tag the module if a concentration of 100 ppm or even 10 ppm were desired. How to bring the pure PFT into the module within the Leak Certification Facility without causing contamination in the zones is a real concern. Also, once in the module, it has to be evaporated and evenly mixed. Because the pure vapors are 14 times the density of air, local overdosing within the module might cause later "hot spots" which could bias leak flow rate calculations.

If a tank of compressed air, pretagged with PFT, is used instead, contamination problems can be greatly minimized. The PFT-tagged air can be added to the module during pressurization for leak checking and then mixed simply within the module with small fans since there is no density difference.

To maintain a comfortable safety factor above the dew point of PDCH at 15°C, the maximum concentration of oPDCH that can be used in a cylinder at 1000 psig is 200 ppm. The type of aluminum cylinder that Brookhaven has been using with PFTs have an air capacity of 76.6 ft^3 NTP at 1000 psig.

For the 7070-ft^3 module, the following quantities of PFT-tagged air would be required from the cylinder:

Conc. oPDCH in module, ppm	1.0	0.1
Dilution ratio	200-to-1	2000-to-1
At 1.1 atm absolute		
Qty of cylinder air, ft^3	38.9	3.89
Percentage of cylinder	50.8	5.08
At 2.0 atm absolute		
Qty of cylinder air, ft^3	70.7	7.07
Percentage of cylinder	92.3	9.23

Thus, one cylinder of the tagging gas would be good for one test at 1 ppm and ten tests at 0.1 ppm.

Minimum Detectable Leak Rates

Equation (B-9) can now be used to estimate the minimum detectable leak rate capability under the conditions given above. For example, for a 60-min duration sample, the following optimized conditions prevail:

$$R_E = 300\ m^3/h$$

$$C_{mi} = 1\ \text{ppm oPDCH} = 0.4\ \text{ppm ocPDCH} \equiv 0.4 \times 10^6\ pL/L$$

$$\text{minimum } v_\ell = 1.20\ fL\ \text{ocPDCH}$$

$$\text{sample V} = 60\ \text{min} \times 0.2\ L/\text{min} = 12\ L$$

Therefore, the minimum $C_\ell = v_\ell/V = 0.10\ fL/L\ (pL/m^3)$ and Eq. (B-9) gives

$$R_\ell = \frac{C_\ell R_E}{C_{mi}} = \frac{(0.10)(300)}{0.4 \times 10^6} = 7.5 \times 10^{-5}\ L/h$$

which is equivalent to a minimum detectable module leak rate of 0.00002 mL/s. Table B-1 shows the results for the above example as well as for a reasonable selection of the range of the variables in Eq. (B-9).

Table B-1

Minimum Detectable Leak Rates at ±12% Uncertainty

Conc. oPDCH in module, ppm	0.1		1.0	
Sampling duration, min, @ 200 mL/min	6	60	6	60
Minimum R_ℓ, mL/s	0.002	0.0002	0.0002	0.00002
L/h	0.0075	0.00075	0.00075	0.000075

The minimum detectable leak rate of 0.00002 mL/s represents about a five order-of-magnitude improvement over the original specification being promulgated. Equation (B-9) can be used to see if the actual capability will meet this expected level. The air leakage rates in the tarpaulin zones, R_E, are not likely to be significantly different from 300 m^3/h. The concentration in the module could be increased to 100 ppm for a 100-fold improvement in leak detection, but it is probably not necessary; concentrations up to 100 ppm are possible if an appropriate tagging concept is developed which would eliminate any chance of contamination or poor mixing. Lastly, the minimum C_ℓ capability is the minimum tracer quantity detectable in the largest possible sample collected. No further improvements are likely in the minimum quantity of tracer detectable, but the amount of sample air collected in 60 min could easily be increased about 10-fold.

Thus, although a five order-of-magnitude improvement in leak detection capability is anticipated, further improvements are possible.

APPENDIX C

PERMEATION THROUGH SEALS: CONSEQUENCE FOR LEAK DETECTION

The limiting factor in leak determinations on a module containing elastomeric or polymeric seals is, possibly, the rate of permeation of the tracer vapors through the seals when the module itself is hermetically tight. However, the permeation of vapors through a seal can take an extensive amount of time to begin emitting and even longer to reach a steady state rate.

The process of permeation is governed by the solubility of the vapor or gas in the seal and its diffusion rate in that materials such that

$$P = S \times D \qquad \text{(C-1)}$$

where P = permeability, 10^{-10} $cm^3 \cdot cm/cm^2$ s cm Hg

S = solubility, cm^3/cm^3 cm Hg

D = diffusion constant, 10^{-10} cm^2/s

When using PFT for leak detection, it is the permeation of the PFT vapors through the seals that may have a limiting effect--not the permeation of air. In this appendix, a simple estimate of the dimension of an elastomeric module seal will be made and the rate of permeability of air and a PFT will by compared to the expected leak.certification capability.of the PFT technology.

SEAL DIMENSIONS AND PERMEABILITY DATA

It was assumed that all the seals on a module comprise an exposed area of 1000 cm^2 (equivalent to about a 33-foot length and a width of 1 cm), a thickness of 1 cm (between the inside cabin air and the vacuum of space), and that the pressure differential was 1 atm (76 cm Hg).

The permeation rates of air through various seal materials at room temperature, available from the literature, are listed in Table C-1. Also shown are solubility and diffusion constant data for one PFT (PMCH) in two materials taken from a previous Brookhaven study[10] along with the computed permeability from Eq. (C-1). The components are listed in decreasing order of permeability, that is, the best seal materials to minimize loss of air from a module are at the bottom of the table.

Clearly, there is a wide range in the permeability of vapors and gases through seal materials. Presumably, a module seal would be selected from components at the bottom of the table. It should be noted that the difference in solubility and diffusion constants for different PFTs, in the same material is small[10]; thus the data shown for PMCH is applicable to the leaking tracer ocPDCH.

Table C-1

Permeability, Solubility, and Diffusion Constant Data[a] at Room Temperature

Seal Material	P(air)	P(PMCH)b	S(PMCH)	D(PMCH)
Fluorosilicone 35	---	600	0.24	2,500
Polyethylene	2.78			
Butyl Rubber	0.52			
PVC	0.056			
Mylan	0.0084			
Viton	0.0072	0.29	0.18	1.6

[a] The units of P, S, and D are given in Eq. (C-1).
[b] Calculated from Eq. (C-1).

PERMEATION RATES AT STEADY STATE AND TIME TO STEADY STATE

Using the earlier assumptions

ΔP = 76 cm Hg (1 atm)
Area = 1,000 cm2
Thickness (l) = 1 cm

the leak rate of air due to permeation ($R_{\ell P}$) through a viton seal is

$$R_{\ell P} = 0.0072 \times 10^{-10} \times 76 \times 1000 / 1 = 5.5 \times 10^{-8}\ cm^3/s = 2.0 \times 10^{-7}\ L/h$$

The leak rate of PMCH due to permeation ($S_{\ell P}$) is, in effect, a source rate which can then be converted to an effective air leak rate by dividing by the assumed concentration in the module, namely,

$$R_{\ell P}(PMCH) = S_{\ell P} / C_{mi}$$

The time to attain steady state (t_{ss}) can be estimated by[10]

$$t_{ss}(s) = \ell^2 / D$$

where l is the thickness (cm) of the seal.

The data in Table C-1 was used in the above equations to calculate the effective leak rates of a module due to permeation through seal materials from Viton (the least permeable) to fluorosilicone 35 (the most permeable) rubber to be compared to the best leak detection capability attainable with the PFT technology of 7.5×10^{-5} L/h as shown in Appendix B.

Presumably the module seals are making use of a material with performance similar to Viton. The direct leak of air via permeation at steady state (2.0×10^{-7} L/h) is almost 400-fold less than is detectable by the PFT technology leak certification approach. The effective leak rate due to permeation of the PFT (assuming a module concentration of 1 ppm) is 7.9×10^{-6} L/h, about 10-fold less than detection capability. In addition, the time for permeation of the PFT to reach steady state is about 200 years. Thus, for a one or 2-day test, effectively no PFT could permeate through a Viton seal.

Although the effective leak rate at steady state for a fluorosilicone 35 rubber seal is much higher (1.6×10^{-2} L/h), its time to reach steady state of 46 days would also preclude detection of permeating PFT in a 1- or 2-day test. The likelihood of using such a permeable rubber is also quite low.

In conclusion, then, permeation through seals on the SSF modules is not of consequence to the leak certification project.

APPENDIX D

PROPOSED SEAL-INTEGRITY CERTIFICATION

Air leaking from a module may occur through a variety of penetrations in the shell due to defects in a seal, contamination on a seal or joint, hairline cracks in a structural component, etc. Because there are many potential sources of leaks, their behavior as a function of pressure differential across the shell of the module may be different.

The hypothesis is presented here that if the magnitude of the zonal module leak rates is measured at three (3) or more pressures from 0.2 to 1.0 atm gage, then the functional dependence on pressure differential can be used to qualify if not quantify the structural integrity of the leak path, regardless of the magnitude of the leak. Thus, a module zone might pass a leak rate specification but fail a seal-integrity certification test. Such testing is possible because, with the PFT approach, a new leak rate versus pressure run can be performed about once every three to five hours.

PRESSURE-DEPENDENCE ON SEAL INTEGRITY

The performance of various types of controlled leaks has been previously studied at Brookhaven. The flow dependence on oxygen pressure for a BNL-developed restrictor device[11] is shown in Figure D-1. The flow dependence on pressure is nearly linear because the restrictor, a solid, 1/16-inch OD stainless steel rod with a slight flat along its edge swaged within a 1/8-inch OD by 1/16-inch ID stainless steel tube, is a high-integrity device. Similarly, the flow rate through a laser-drilled jeweled-orifice was found to be very linear with pressure (cf. Figure D-2); such a leak device would have high dimensional stability with changing pressure.

Brookhaven also developed a diffusion leak rate device consisting of a 40 Å porous glass wafer held in place by PVC flat rings within a 1/8-inch compression fitting.(12) A plot of the logarithm of flow rate versus the logarithm of CO pressure shows a power pressure dependence of just slightly greater than unity, implying excellent seal integrity over the range of pressures from 4 to 200 psig (cf. Figure D-3).

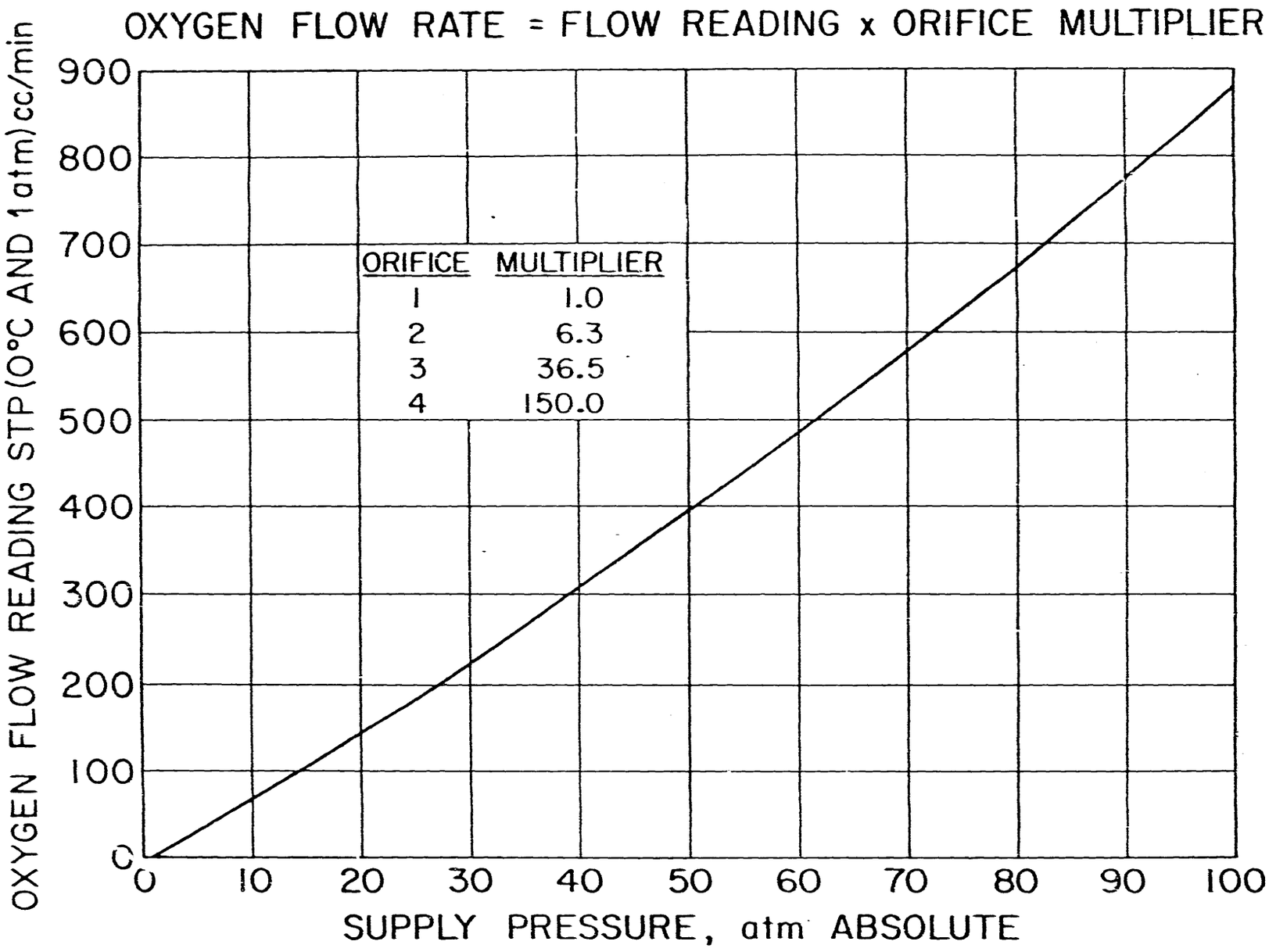

Figure D.1. Oxygen flow rate versus pressure through a Brookhaven restrictor device.

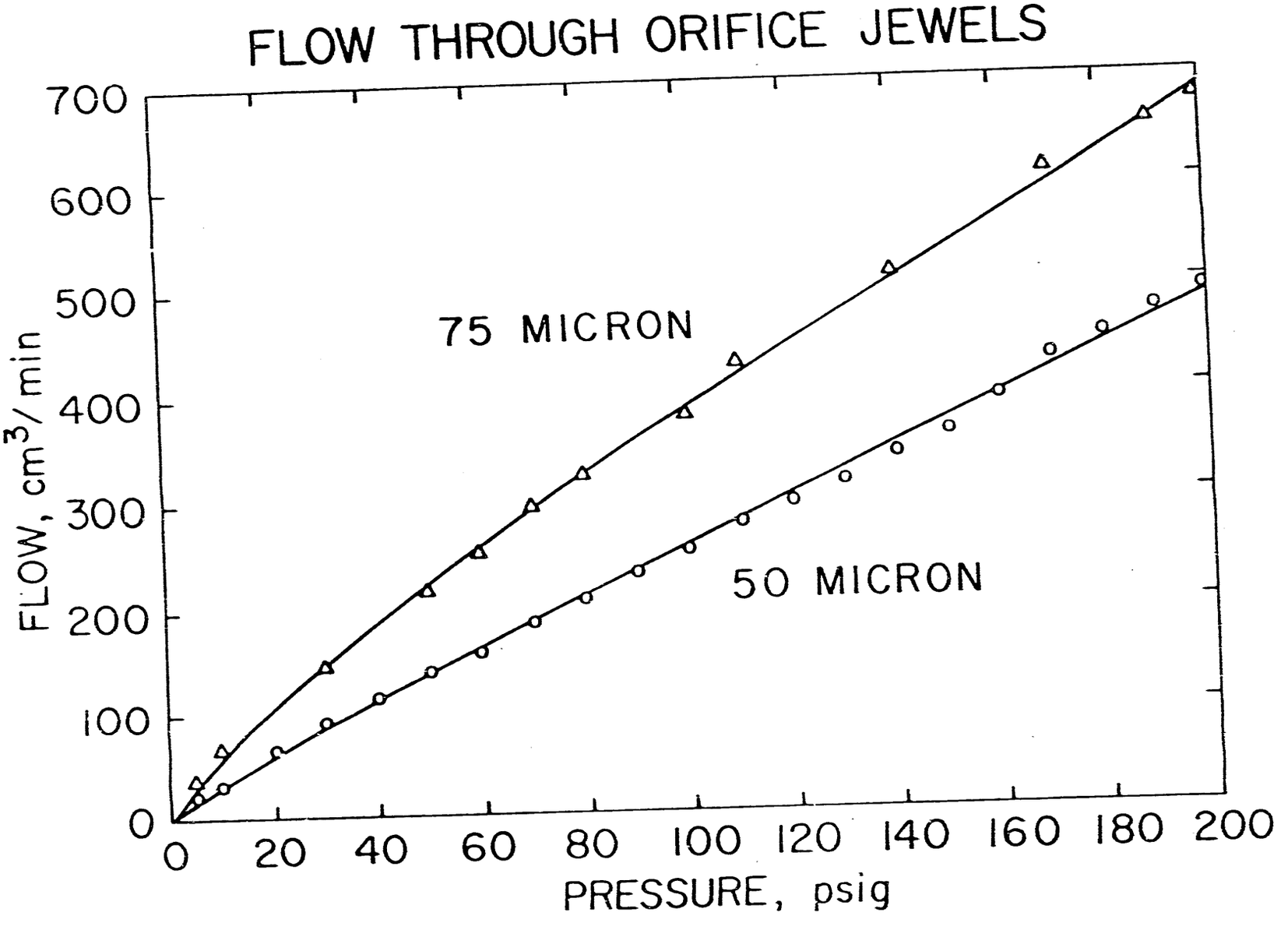

Figure D.2. Flow versus pressure differential through a jeweled-orifice.

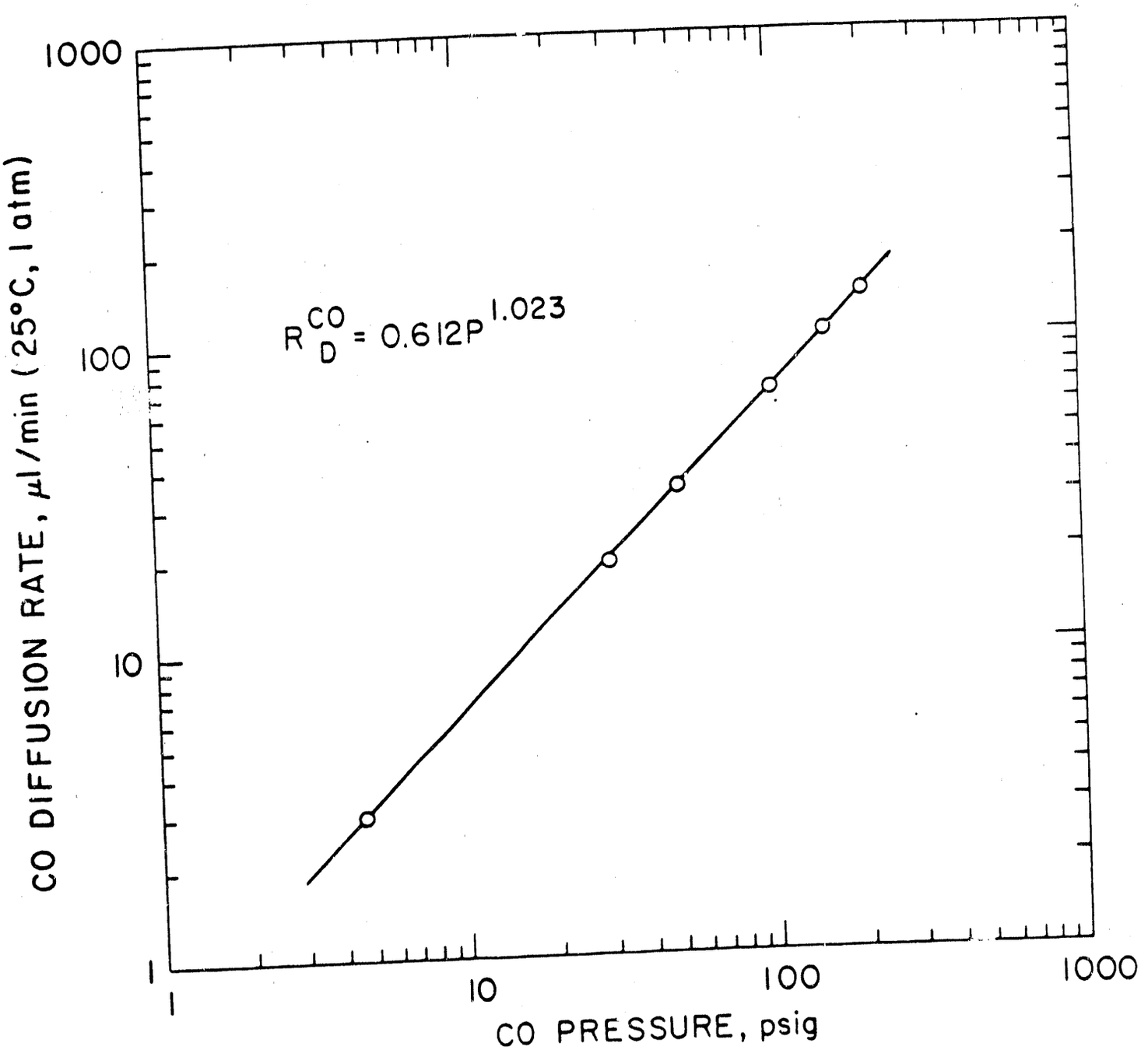

Figure D.3. Logarithm CO flow versus logarithm ΔP through a porous glass wafer.

Another device, a capillary tube rolled in a drawing tool to further reduce its diameter, was used to control CH_4 flow rates. The calibration data obtained by measuring the volume of CH_4 diffused as a function of time[13] is shown plotted in Figure D-4 for several pressures. The calculated flow rates were then plotted as a function of pressure differential on a log-log plot (cf. Figure D-5), which gave a power pressure dependence of 1.649 imply a dimensional dependence on pressure.

Also shown in Figure D-5 are the flow rate performance of two other devices. The oxygen through the restrictor is the data of Figure D-1 showing a power dependence on pressure of only 1.068, imply good dimensional stability. The dashed line in Figure D-5 is the data for a restrictor device that was intentionally made poorly. Indeed, the flow rates' dependence on pressure increased with pressure implying poor structural integrity.

The five devices are listed in Table D-1 arranged in order of decreasing leak rate at 14.7 psig from 2.1 down to 0.00057 L/h, about in the range of module leak certification. However, it can also be seen that the magnitude of the leak rates does not influence the power dependence which was essentially units for the first two and the last device; the third and fourth devices had bad and poor performance, respectively, implying a structural integrity problem.

Table D-1

Leak Rate Devices and their Dependence on Pressure

Device	Leak Rate at 14.7 psig, L/h	Power Dependence on Pressure	Implied Integrity
Jewel Orifice	2.1	1.0	Excellent
Restrictor	0.38	1.068	Good
Poor restrictor	< 0.005	1.5 to 2.5	Bad
Capillary	0.00088	1.649	Poor
Porous glass	0.00057	1.023	Very good

Pressure difference, of course, can create large forces on vessels containing seals. The jeweled-orifice and the porous glass device inherently have excellent integrity; glass cannot be deformed by these pressures, only the seals used to contain the glass, which is why the power dependence is not exactly 1. The capillary tube and the restrictor, having been fashioned of expandable stainless steel

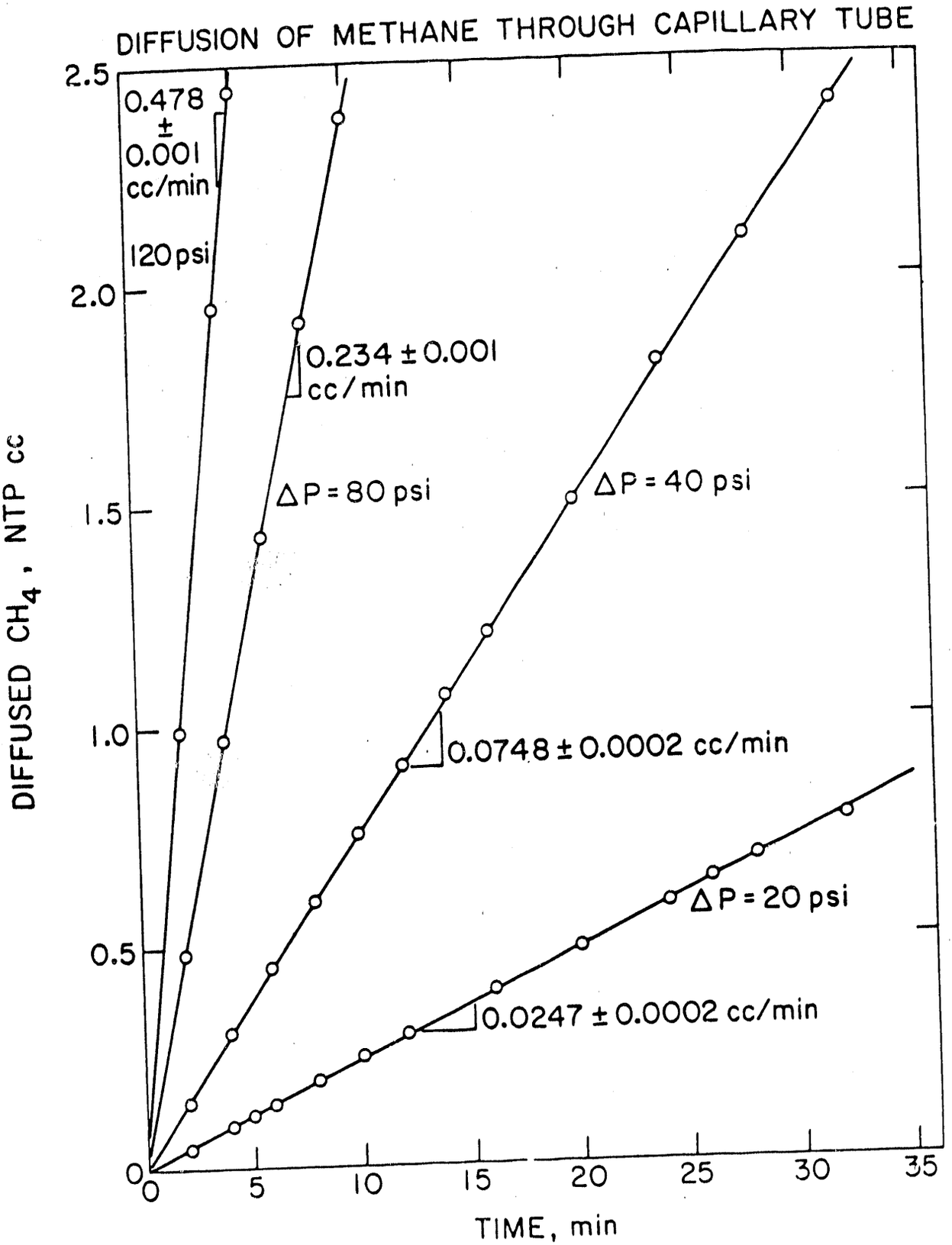

Figure D.4. Quantity of CH_4 diffused versus time for a capillary tube orifice.

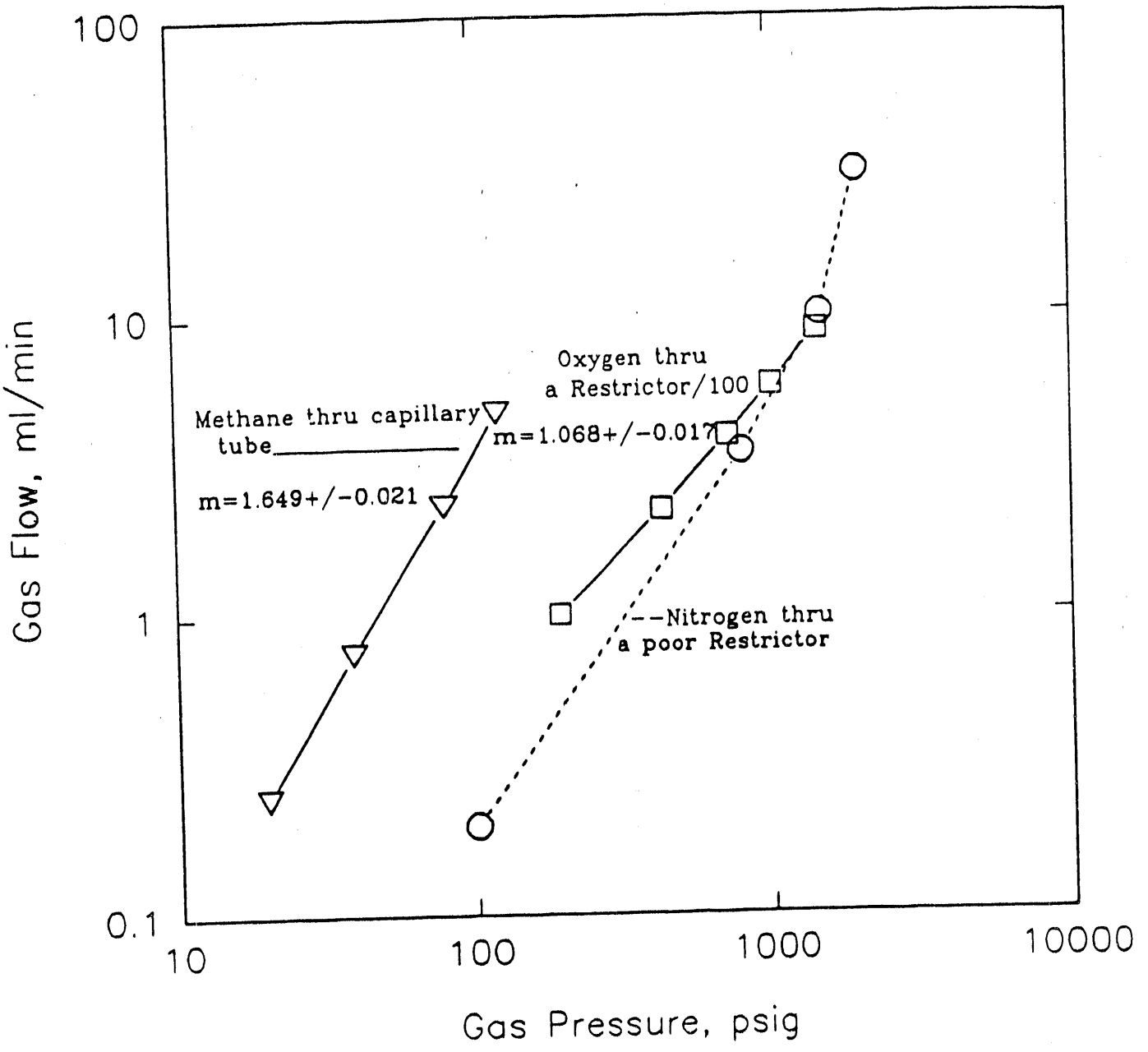

Figure D.5. Logarithm flow rate versus logarithm ΔP.

components, are showing the effects of the pressure forces on changing its dimension (opening increases with pressure).

For a restrictor of 1/16-inch ID and a module 15-ft in diameter, the radial surface area and force per linear inch at their respective operating pressures are

	Restrictor (1/16-inch ID)	Module (15-ft ID)
Circum. Surface Area, in.2/in	0.20	565
Operating DP, psig	2000	14.7
Force, lbs/linear in.	390	8,300

Even though the maximum operating pressure of the pressure-dependent restrictor (2000 psig) is much higher than that of a module (14.7 psig), the forces on the latter are much larger, making it quite likely that the dependence of leak rate on pressure differential will have a power factor significantly greater than unity for even the small flow in structural integrity of the seal.

OTHER FORCES AFFECTING SEAL INTEGRITY

Pressure results in just one force that might influence the integrity of module seals and result in large variations in leak rates as a function of pressure. Any force which can move one surface of the module with respect to another surface could result in a change in the dimensions of a leak path.

Parameters such as vibrations and torque (which can be produced during shipment, placement in orbit, during docking maneuvers, etc.), temperature fluctuations (such as going from ground to space environments, changing solar gain, etc.), and load distribution could create significant forces which could result in large variations in the magnitude of leak rates.

The proposed Leak Certification Facility should include the capability to create some of these forces while measuring the leak rates dependence on pressure using the PFT technology. Such seal integrity testing will greatly enhance the safety and reliability of the SSF modules. These same techniques could also be applied to seal integrity testing in many other NASA applications, such as engines, solid rocket boosters, fuel and oxidant lines, etc.

END

DATE FILMED

7/8/92